

Journal of Pharmacy and Chemistry

(An International Research Journal of Pharmaceutical and Chemical Sciences)
Indexed in Chemical Abstract and Index Copernicus (IC Value 5.28)

www.stfindia.com
www.jpc.stfindia.com

Editor-in-chief

Prof. K.N. JAYAVEERA
*Jawaharlal Nehru Technological University Anantapur,
Anantapur, Andhra Pradesh -515001.*

Executive Editor

Dr. K. Balaji

Editorial Board

Dr. B.M. Vrushabendra Swamy	Dr. A. Venkateshwar Reddy
Dr. G. S. Kumar	Prof. T. Ram Mohan Reddy
Dr. S. Subramanyam	Dr. K. Yogananda Reddy
Dr. K. Bhaskar Reddy	Dr. K. Adinarayana
Dr. K.V. Madhusudhan	Dr. A. Sunil Kumar Reddy

Editorial Advisory Board

Prof. Nagarapu Lingaiah	India	Prof. G. Krishna Mohan	India
Prof. T.R. Rao	India	Prof. M.L.N.Rao	India
Prof. R.Nageshwara Rao	India	Prof. S. Srihari	India
Prof. K.V.S.R.G. Prasad	India	Prof. K.V. Ramana Murthy	India
Prof. K. Kannan	India	Prof. Yeoh Peng Nam	IMU, Malaysia
Prof. D.R. Krishna	U.S.A	Prof. M. Kalilullah	India
Prof. Jonathan R Dimmock	Canada	Prof. Ananth. P. Haridas	India
Prof. Helton Max M. Santos	Portugese	Prof. Damaris Silveira	Brazil
Prof. Mustafa Iraz	Turkey	Prof. Abdul Naser B Singab	Egypt
Prof. Ali Asgarh hemmati	Iran	Prof. N. Devanna	India
Prof. K.R.S. Sambasiva Rao	India	Prof. R. Shyam Sunder	India
Dr. Nitin Mahukar	India	Prof. Arun Goyal	India
Prof. Sarangapani	India	Prof. Sunil.K.Khare	India
Prof. Y. Narasimha Reddy	India	Dr. S.Narasimha Murthy	U.S.A
Dr. Girish Gowda	Saudi Arabia		

Journal of Pharmacy and Chemistry

(An International Research Journal of Pharmaceutical and Chemical Sciences)

Volume 8 • Issue 1 • January – March 2014

Contents

Cytokinin Like Effect of Bisphenol-a on Oxidative Metabolism in Mung Bean Seedlings	3
K. PADMAJA, P. ESWARA PRASAD AND K. JAYASRI	
Physical Properties of Sputtered TiO₂ Thin Films.....	7
M.THAIIDUN, B.VENKATA RAO, L.RAJA MOHAN REDDY, AND C.BALANARAYANA	
Formulation and Evaluation of Sustained Release Matrix Tablet	10
Y.NAGA LAXMI, P.AMARESHWAR, S.MAANASA, M.V.RAMANA, AND P.SRAVANTHI	
Formulation and Evaluation of Fast Dissolving Tablets of Poorly Water Soluble Drug.....	18
S. MAANASA, P. AMARESHWAR, Y. NAGA LAXMI, M.V. RAMANA, AND P. SRAVANTHI	
Zirconia Supported Phosphotungstic Acid Mediated Synthesis of Homoallylic Alcohols	24
SANNITHI SURESH BABU, C.V. HARIHARAKRISHNA, AND K. MUKKANTI	
Synergistic and Individual Neurotoxicity of Fenvalerate and Azadirachtin on Atpases Activity in the Cockroach, Periplaneta Americana	28
D. ARUNA KUMARI, K.V. MADHUSUDHAN, S. GOPAL AND G. RAJARAMI REDDY	
Design and Development of Transdermal Patches for Verapamil Hydrochloride	35
P. SRIKANTH REDDY, D. SARITHA, M. RAVI KUMAR AND K.N. JAYAVEERA	
INSTRUCTION TO AUTHORS	44



VIEWS

The views and opinions expressed in this journal are those of the contributors; Science-Tech Foundation does not necessarily concur with the same. All correspondence should be addressed to the Editor-In-Chief (Hon.), Journal of Pharmacy and Chemistry (Science-Tech Foundation), Plot No 22, Vidyut Nagar, Anantapur - 515 001, Andhra Pradesh, India. • e-mail:editorjpc@gmail.com. **Send your queries at www.jpc.stfindia.com, www.stfindia.com**

Cytokinin Like Effect of Bisphenol-a on Oxidative Metabolism in Mung Bean Seedlings

K. PADMAJA, P. ESWARA PRASAD AND K. JAYASRI

Department of Veterinary Biochemistry, College of Veterinary Science,
Sri Venkateswara Veterinary University. Tirupathi, A.P.

ABSTRACT

Bisphenol-A is identified as a potential reproductive and developmental toxin as well as hormone disturbing chemical leading to a variety of health effects. BPA has been shown to exert estrogenic effects in animals, however its biochemical effects on plants were not studied widely. The present work was aimed to elucidate the mechanism of action of bisphenol-A at different concentrations on oxidative metabolism and on chlorophyll levels during different days of germination period in Mung bean seedlings. Results showed that MDA levels decreased with increasing concentrations of Bisphenol-A and there was 32% & 52% reduction on 3rd day of germination at 0.4mM and 0.7mM BPA concentration respectively. Further BPA treatment showed increased activity of antioxidant enzymes such as SOD, CAT & GPx and non enzymatic antioxidants such as Glutathione and Carotenoids. An induction in chlorophyll and protein levels with increasing concentrations of Bisphenol-A was also observed.

Key Words: Bisphenol-A, Oxidative stress, Chlorophyll, Antioxidant enzymes.

Introduction

Bisphenol-A (BPA:2,2 bis 4-hydroxy phenyl propane) is an important industrial chemical extensively used as a monomer in the fabrication of hard and transparent polycarbonate plastics, epoxy resins and unsaturated polyester-stryene and is used in all such as infant feeding bottles, food and drink packaging, electrics and electronics etc.(1). BPA is synthesized to a tune of about 3.7 million tonnes/year world wide. As a result BPA contamination in the environment was repeatedly confirmed in the waste water effluents, raw sewage & sewage sludge. Since agriculture soils are often enriched with activated sewage sludge, biosolids that may contain BPA, organisms dwelling in the soil and of course rooted plants could encounter BPA from that source (2). Hydrolysis of ester bonds of plastic polymers of food and beverage packing or storage containers can potentially release BPA into food stuffs and beverages and therefore be digested raising great concern about the possible hazards for consumers(3).

Plants and seedlings can rapidly absorb BPA through their roots from water and translocate it to their leaves (4). The highest amount of oxygen in plant cells are formed in chloroplasts, and mitochondria. Toxic byproducts of aerobic

metabolism and partially reduced or activated derivatives of oxygen (H_2O_2 , O_2^-) are highly reactive and can lead to oxidative destruction of cells, which in turn leads to impairment of various physiological and biochemical processes in the cell. Plants can respond to stress through their anti-oxidant system which is composed of non-enzymatic antioxidants such as Glutathione (GSH), Carotenoids (5) and enzymatic antioxidants such as Super oxide dismutase (SOD) capable of destroying the O_2^- and of transforming into H_2O_2 which later will be eliminated by the action of Catalase (CAT) and Glutathione peroxidase (GPx). Seedlings are used to test tolerance because of their high sensitivity to toxins during the germination stage (6).

Materials and Methods

Seeds of Mung bean (*Phaseolus vulgaris L.*) were obtained from Andhra Pradesh State Seed Corporation and healthy seeds were washed thoroughly with tap water, allowed to imbibe in water for 5hr and spread over moist filter paper in Petri dishes. Controls were maintained with distilled water and other lots of seeds were treated separately with 0.4mM (T_1) and 0.7mM (T_2) concentrations of BPA dissolved in distilled water. Seedlings were maintained under natural day light (12h) for 4 days at day and night temperatures of $30\pm 2^\circ C$. Seedlings removed on 3rd and 4th day of germination and were used for the experiments.

*Address for correspondence:

Five replicate experiments were conducted to obtain the results. Analysis of the parameters was carried out as Chlorophyll content by Arnon (7), Carotenoids by Lichtenthaler, H.K (8), lipid peroxides as thiobarbituric acid (TBA) reaction by Heath and Packer (9), SOD activity was according to Misra and Fridovich (10), Catalase activity was of Beers and Sizier (11), Protein content was by Lowry *et al.*, (12), Glutathione peroxidase activity by Rotruck *et al.*, (13), Glutathione was by Ellman(14).

Results

Increased chlorophyll and carotenoid levels were observed with BPA treatment. The percentage of increase in carotenoid levels was 53% and 70% on 4th day with 0.4mM & 0.7mM concentration respectively. Chlorophyll levels increased to 40% & 46% on 3rd day with 0.4mM & 0.7mM concentration of BPA respectively (Table.1).

Increasing concentrations of BPA decreased MDA levels and it was found to be 32% & 52% reduction on 3rd day at 0.4mM and 0.7mM concentrations respectively. Whereas, it was reduced to 74% with 0.7mM of BPA concentration on 4th day of germination. Significant induction in GSH levels observed on 4th day compared to 3rd day and it was 56% and 60% on 4th day compared to 22% and 50% on 3rd day with 0.4mM & 0.7mM concentration of BPA respectively (Table. 2)

Significant induction in SOD and CAT activities with increasing concentrations of BPA was observed. The percentage of induction in SOD activity is 41% & 77% on 3rd day and 45% & 60% on 4th day with 0.4mM and 0.7mM concentration of BPA respectively. CAT activity increased significantly to 36% & 47% on 3rd day with 0.4mM & 0.7mM of BPA concentration respectively (Table.3)

Table-1
Effect of Bisphenol-A on Chlorophyll and Carotenoid levels

Parameter	3rd day			4th day		
	C	T ₁	T ₂	C	T ₁	T ₂
Chlorophyll (mg/g wt)	0.57 ± 0.005	0.95*± 0.003	1.05*± 0.016	1.81 ± 0.013	2.20* ± 0.46	2.42* ± 0.13
Carotenoids (mg/g wt)	0.15 ± 0.003	0.17*± 0.007	0.19*± 0.008	0.85 ± 0.03	1.84* ±0.042	2.8* ±0.06

Values are mean concentrations ± SD p<0.001

Table-2
Effect of Bisphenol- A on MDA and GSH levels

Parameter	3rd day			4th day		
	C	T ₁	T ₂	C	T ₁	T ₂
MDA (μ moles/g wt)	55.45± 0.44	37.42*± 0.41	26.6*± 0.24	29.6± 0.49	27.08*± 0.36	7.68*± 0.22
GSH (mg/g wt)	0.12± 0.002	0.15*± 0.001	0.23*± 0.008	0.35± 0.002	0.80*± 0.003	0.87*± 0.003

Values are mean concentrations ± SD p<0.001

Table-3
Effect of Bisphenol A on SOD and Catalase activities

Parameter	3rd day			4th day		
	C	T ₁	T ₂	C	T ₁	T ₂
SOD (units/ mg protein)	0.021± 0.001	0.034*± 0.002	0.090± 0.001*	0.022± 0.002	0.040*±0.002	0.050*±0.002
Catalase (units/ mg protein)	0.32± 0.004	0.51*± 0.01	0.62*± 0.01	1.56± 0.04	2.38*± 0.06	2.76*± 0.09

Values are mean concentrations ± SD p<0.001

GPx activity increased on 4th day to 22% and 49% with 0.4mM and 0.7mM concentration of BPA respectively (Fig.1). Increased levels of protein observed with increasing concentration of BPA both on 3rd and 4th day whereas maximum protein induction was observed with BPA treatment on 3rd day (Fig.2).

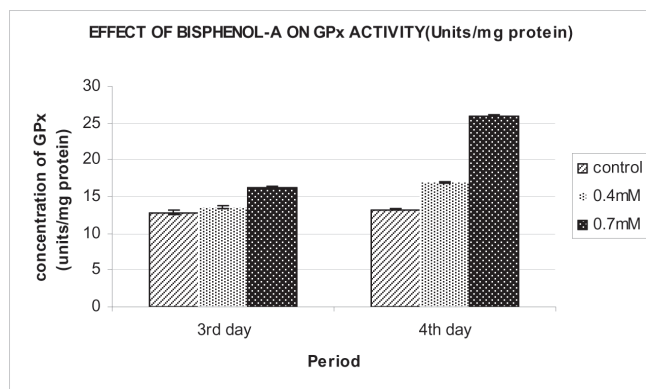


Fig. 1. Effect of BPA on GPx activity
Values are mean \pm SE $p < 0.001$

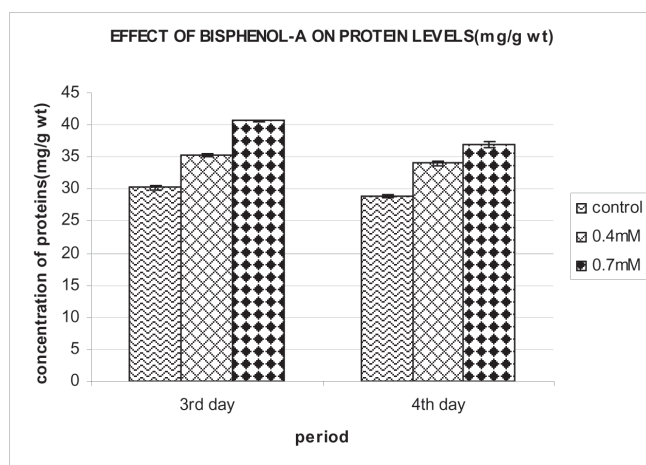


Fig. 2. Effect of BPA on protein levels
Values are mean \pm SE $p < 0.001$

Discussion

Chlorophyll content is an extremely important parameter in estimating the plant production level. One of the sources of ROS is the chloroplasts because of the photoactive nature of chlorophyll (15). Adverse effect on chlorophyll synthesis ultimately reduced photosynthetic activity. Inhibition of this pathway also leads to the accumulation of tetrapyrrole intermediate products. These intermediates readily excite upon illumination and interact with molecular oxygen to generate ROS. To reduce the production of ROS, plants developed various enzymatic and non enzymatic protective mechanism.

BPA driven acceleration of tetrapyrrole metabolism results in stimulated chlorophyll biosynthesis (16). It was already reported that BPA shows cytokinin like activity on growth and shoot differentiation in plants (17). Chloroplasts are among the main targets of cytokinin action in plant

cells. Numerous plant developmental processes have been found to be influenced by cytokinin like inhibition of leaf senescence (18). Exogenous application of cytokinin increased chlorophyll content, because cytokinins promote conversion of etioplasts into chloroplasts via stimulation of chlorophyll synthesis. Increased chlorophyll content with BPA treatment may be due to cytokinin like action.

Carotenoids are organic pigments found in chloroplasts. Chemically they are tetraterpenoids. They absorb light energy for use in photosynthesis and protect chlorophyll from photodamage. Carotenoids are efficient free radical scavengers. Most of the carotenoids have antioxidant activity. Increased levels of carotenoids with BPA treatment are responsible for reduction in oxidative damage.

Lipid peroxidation refers to the oxidative degradation of lipids. MDA, a cytotoxic product of lipid peroxidation has been proposed as a suitable marker of lipid peroxidation(19). Cytokinins can also participate in removal of ROS from the cell, showing direct antioxidant activity. Treatment with cytokinin has the potential to reduce oxidative stress in plants which may be the reason for reduction in MDA formation with BPA treatment. A decrease in the MDA formation was also observed in wheat plants exposed to N- deficiency and treated with exogenous CKs (20). Lack of induction of LPO in the plants during BPA treatment support the cytokinin like activity.

Glutathione in plant chloroplasts play an important role in protecting the photosynthetic apparatus from oxidative damage. Most of the non protein -SH groups in plants represent glutathione which is ubiquitous thiol containing tripeptide which plays an important role as an antioxidant to scavenge ROS through the oxidation of GSH to GSSG. Our results are in accordance with earlier reports which show that increased synthesis of GSH under different types of stress would prompt more tolerance of the plant against stress (21).

Further the level of antioxidant enzymes may also determine the sensitivity of plants to lipid peroxidation. Antioxidant enzymes like CAT, SOD and GPx have been identified as the enzymatic protectors against peroxidation reactions (22). Increased activity of GPx observed with BPA treatment similar to Goran *et al.*, (20). The activities of SOD and CAT increased with the age of the seedling, because they provide an effective mechanism for the removal of free radicals from the cells. It was found that cytokinins can increase the activity of antioxidant enzymes and therefore delay the senescence of the plant tissue (23).

Increased levels of protein observed with BPA treatment because hydroxyl radicals which are responsible for destruction of proteins are not produced with treatment. Our results are in consistent with Grill *et al.*, (22). It was already reported that cytokinin promotes the tetrapyrrole biosynthetic pathway during plant development, protein contents and enzyme activities (24).

Earlier reports together with the results presented here showing the lack of induction of lipid peroxidation with BPA treatment during germination stage support the notion of a role of cytokinins. The absence of oxidative stress was also indicated by increased activity of antioxidant enzymes such as SOD, CAT & GPx and non enzymatic antioxidants such as glutathione and carotenoids. The elevated chlorophyll levels correlate the sharp decrease in MDA formation with BPA treatment. All these results further biochemically confirm that BPA shows cytokinin like activity in plants during germination.

References

1. Staples C A, Dome P B *et al.*, Chemosphere.1998; 36:2149.
2. Ike M, Jin C S and Fujita M. Water Sci.Technol.2000; 42:31.
3. Kang J H, Katayana Y and Kond F. Toxicology.2006; 217, 81.
4. Dogan M, Yumutas.O *et al.*, J.Agric& Environ. Sci. 2010; 9(2):186.
5. Cameron A C and Reid M S. Biol. Technol.2001; 22:169.
6. Parkpain P, Leong S T *et al.*, Environ.Monit.Assess. 2002; 74:27.
7. Arnon D L. Plant Physiol. 1949; 24:1.
8. Licutethaler H K. Mech.Enzynol.1987; 148: 350.
9. Heath R L and Packer L. Arch. Biochem. Biophys.1968; 125:189.
10. Misra H P and Fridovich. Ind J.Biol.Chem.1972; 247:3170.
11. Beers R F and Sizer I W. J.Biol. Chem.1952; 195:133.
12. Lowry O H, Rosebrough N J *et al.*, J.Biol. Chem.1951; 193:265.
13. Rotruck J T, Pope A C *et al.*, Science.1984; 179: 588.
14. Ellman G L. Biochem. Biophys.1959; 82. 70.
15. Asada K and M Takahashi. Elsevier, Amsterdam.1987:227.
16. Aneta Sabovjevic, Marko Sabovjevic *et al.*, Period. Biolog. 2010; 112:301.
17. Nobuyuki Terouchi, Kuniko Takano, Plant Biotech.2004; 21 (4), 307.
18. Pospisiova.J, Synkova.H and Rulcova.J. Biologia plant. 2000; 43(3): 321.
19. Christophe B, Abdelilan B *et al.*,Physiol.Plant.1996;97 :104.
20. Goran Z, Stoparic I V Maksimovic. Pro.Nat. Sci.2008; 114, 59.
21. Monk L S, Fagerstedt.K V & Crawford R M M. Physiol. Plant.1989; 76:456.
22. Grill D H Esterbauer and Klosch U. Environ.Pollut.1979; 19:187.
23. Haliwell B. Chem. Phys. Lipids. 1987; 44: 327.
24. Yaronskaya E, Vershilovskaya I *et al.*, Planta August.2006 ; 224:700.



Physical Properties of Sputtered TiO₂ Thin Films

M.THAIDUN^{1*}, B.VENKATA RAO¹, L.RAJA MOHAN REDDY¹, AND C.BALANARAYANA¹

Department of Physics, Loyola Degree College (YSRR), Pulivendla, A.P., India. 516390

ABSTRACT

Thin films of TiO₂ were deposited on quartz and p-Si (100) substrates held at room temperature by sputtering of titanium target at various sputter powers in the range 80 - 200 W. The as-deposited films were annealed in air for an hour at 1023 K. The annealed films were characterized by using Fourier transform infra red spectroscopy, X-ray diffraction, Surface morphology, dielectric and optical properties. The deposition rate of the films increased from 1.26 to 6.66 nm/min. with increase of sputter power from 80 to 200 W. TiO₂ films formed at sputter power of 80 W and annealed at 1023 K were polycrystalline in nature with anatase phase crystallite size of 40 nm, dielectric constant of 10, optical band gap of 3.65 eV and refractive index 2.35.

Keywords: TiO₂, Sputtering.

Introduction

The development of TiO₂ thin films is of particular interest due to the numerous technological applications of this inorganic oxide. Metal oxide semi conducting materials appear to be one of the best candidates for gas sensing, as they operate reversibly and usually have stable chemical and thermal properties over extended periods of use [1]. TiO₂ thin films are popular for such applications, where changes in the film electrical conductivity can be related to the physisorption and chemisorption of oxygen atoms [2, 3]. Titanium dioxide has many excellent physical properties such as a high dielectric constant, a strong mechanical and chemical stability, as well as good insulating properties. Due to its high refractive index and optical transmittance in the visible range, TiO₂ is especially suitable as material for optical coating and protective layers for very large-scale integrated circuits [4]. In the last decade, titanium dioxide has also attracted a great deal of interest due to its photo-catalytic behavior [5, 6]. The decomposition of organic compounds on the surface of TiO₂ and the reduction of the contact angle between water and the surface of TiO₂ under UV irradiation results in self-cleaning and anti-fogging effects [7]. It is well known that titania exhibits three distinct crystalline forms apart from the amorphous form: an orthorhombic one, the brookite and two tetragonal phases, the anatase and the rutile [8, 9]. The occurrence of anatase and rutile phase depends significantly on the method and conditions of deposition as well as the substrate temperature [10]. Each crystalline form is convenient for a

different purpose. While rutile is mainly desirable for optical applications, anatase has more efficient photocatalytic properties. Which structure is formed during the fabrication of TiO₂ thin films depends on the deposition technique, the deposition parameters and the deposition configuration.

TiO₂ films were prepared by various methods, such as chemical vapour deposition, pulsed laser deposition, sol-gel deposition, spray pyrolysis, plasma enhanced chemical vapour deposition and DC/RF magnetron sputtering [11-15]. However for most deposition techniques, a high temperature by use of substrate heating or post-deposition annealing is required for the growth of anatase or rutile phases of TiO₂ thin films instated of amorphous films. Compared to other deposition methods, DC Magnetron sputtering technique has significant importance because it enables control of the structure, good adhesion on the substrate of deposited films, high density and homogeneity, composition and properties of TiO₂ films by adjusting the deposition conditions. This results in high quality thin films with thickness uniformity over large areas and well controlled stoichiometry.

Experimental

Thin films of TiO₂ were deposited on silicon and quartz substrates by sputtering of titanium target under various oxygen partial pressures using the DC modes. The TiO₂ films were deposited at oxygen partial pressure of 5×10^{-2} Pa and at a fixed substrate temperature of 303 K and at different sputtering powers in the range 80 – 200 W. The as-deposited films were annealed in air at 750°C for 1 hour. In order to study the dielectric properties of the titanium dioxide films, the MOS capacitor with the structure of metal/

*Address for correspondence:
muttukuri.thaidun@gmail.com

oxide/semiconductor (Al/TiO₂/p-Si) was fabricated. The TiO₂ films were deposited on p-type silicon substrate by DC magnetron sputtering and the top electrode of aluminum was deposited using Hind High Vacuum coating unit by vacuum evaporation. The Si wafers were placed in Teflon container. Insoluble organic contaminants in the wafer can be removed by immersing the wafers in the organic clean solution, which is maintained (5:1:1, H₂O: H₂O₂: NH₄OH) for 10 minutes. Removed carrier from the organic clean solution and rinse wafer in the deionized water for one minute. Submerge the carrier with wafer in the oxide strip solution (50:1, H₂O:HF) for 15 seconds in order to remove silicon dioxide that may be accumulated as a result of organic clean. Then remove carrier from the bath and rinse the wafer in deionized water for one minute. Finally removed the substrates from the substrate carrier contained deionized water and blown dry with nitrogen. The deposited films were characterized by studying the chemical binding configuration using Fourier transform infrared spectroscopy, electron core level binding energies with X-ray photoelectron spectroscopy, electrical and dielectric properties from current-voltage and capacitance-voltage measurements.

Result and Discussion

Figure 3.1 shows the X-ray diffraction profiles of the films formed at different sputtering powers. TiO₂ films deposited at room temperature (303 K) were of X-ray amorphous. The as-deposited films were annealed in air for 1 hour at 1023 K. During DC reactive magnetron sputtering, the particles generally impinge on the substrate with energy in the range of 1–10 eV [16], which accelerates the growth of sputtered TiO₂

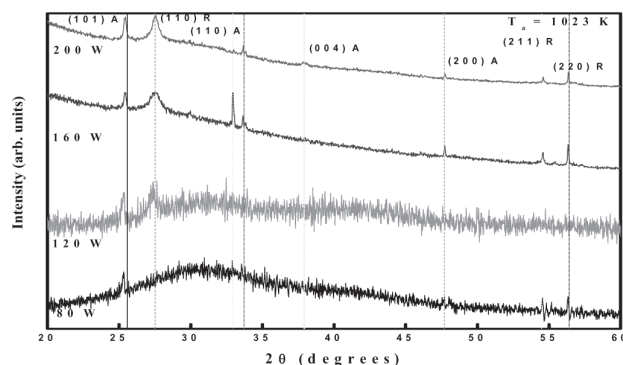


Fig. 3.1: XRD profiles of TiO₂ films at different sputter powers

films with anatase or rutile phase [17]. The films formed at low sputtering power of 80 W showed four weak diffraction peaks were obtained (101), (110), (004) and (200) reflections at $2\theta = 25.24, 33.1, 38.02$ and 47.7° with low intensity indicated the growth of TiO₂ with anatase phase [18]. It indicated that the films formed at 80 W and annealed at 1023 K were polycrystalline in nature with anatase phase of TiO₂. As the sputtering power increased to 120 W, in addition to these peaks another diffraction peaks was obtained (110) planes at $2\theta = 27.3^\circ$ related to the rutile

phase of TiO₂ indicated the presence of mixed phase [19]. The intensity of the reflections (101) was decreased with the increase of sputtering power from 120 to 200 W indicated the decrease in anatase phase TiO₂. The full width at half maximum was decreased related to the (101) plane of anatase phase of TiO₂ with the increase of sputtering power indicated the decrease in crystallite size. The intensity of (110) peak is increased and FWHM decreased with the increase in sputtering power from 120 to 200 W indicated the growth of rutile phase at higher sputter powers. The crystallite size of the films was calculated using Debye-Scherrer's equation

$$L = 0.89 \lambda / \beta \cos\theta \quad \dots (1)$$

Here, λ is the wavelength of the X-rays, β the full width at half maximum intensity of the peak and θ the Bragg diffraction angle. The crystallite size of the anatase TiO₂ films decreased from 40 to 20 nm with the increase of sputter power from 80 to 200 W. And the crystallite size of the rutile phase TiO₂ films were increased from 10 to 30 nm with the increase of sputter power in the range 80 – 200 W.

Fourier transform infrared spectra (FTIR) of TiO₂ films deposited at different sputtering powers are shown in figure 3.2. The FTIR spectra of the films deposited at low sputtering power of 80 W showed a broad absorption band at 438 cm⁻¹ related to the stretching vibration of Ti-O-Ti in anatase phase TiO₂ [20]. When sputter power increased to 120 W, the absorption bands at 494 and 668 were observed with minimum intensity. The band situated at 494 and 668 cm⁻¹ related to the rutile phase vibrational mode of TiO₂ [21]. Further increase of sputtering power to 160 W, the intensity of the bands at 494 and 668 cm⁻¹ were increased indicated the growth of rutile phase TiO₂. The absorption band seen at 438 cm⁻¹ was decreased with the increase of sputtering power indicated the anatase phase TiO₂ decreased with the increase of sputtering power. These results are well supported to the X-ray diffraction studies.

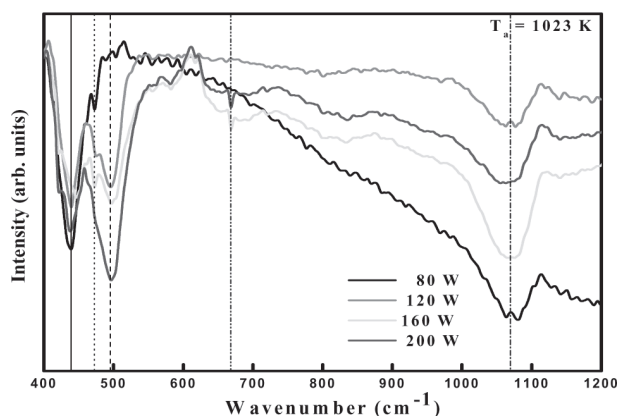


Fig. 3.2 : FT IR spectra of TiO₂ films formed at different sputter powers

The dielectric constant was calculated from the capacitance - voltage curves using the following formula,

$$C = k\epsilon_0 A / t \quad \dots (2)$$

Where C is the capacitance, k the dielectric constant of the material, ϵ_0 the permittivity of free space (8.85×10^{-12} F/μm), A the area of the capacitor, and t the thickness of the dielectric. The dielectric constant of the TiO₂ films formed at sputter power of 80 W was 10 and it increased to 35 with the increase of sputtering power to 200 W. Figure 3.3 shows the dependence of dielectric constant on sputter power. The dielectric constant of the films increased with the increase of sputter power. These annealed films at different sputter powers leads to decrease of structural defects, and change the phase transformation from anatase to rutile phase, hence enhance in the dielectric constant of the TiO₂ films.

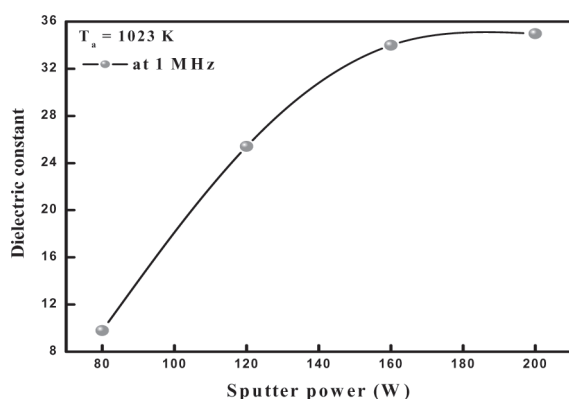


Fig. 3.3 Variation of dielectric constant with sputter power

The refractive index (n) of the films was determined from the optical transmittance interference data employing Swanepoel's envelope method [22] using the equation:

$$n(\lambda) = [N + (N^2 - n_0^2 n_1^2)^{1/2}]^{1/2} \quad \dots (3)$$

$$N = 2n_0 n_1 [(T_{\max} - T_{\min}) / T_{\max} T_{\min}] + (n_0^2 + n_1^2) / 2 \quad \dots (4)$$

where T_{\max} and T_{\min} are the optical transmittance maximum and minimum respectively. The variation of refractive index (at 500 nm) as a function of sputtering power is shown in figure 3.4. The refractive index of the films at the wavelength of 500 nm decreased from 2.48 to 2.35 with the decrease of sputtering power from 200 to 80 W respectively. The low value of refractive index of the films formed at low sputtering power of 80 W was due to the single phase TiO₂ films. The high value of refractive index in the films formed at high sputtering power 200 W was due to the presence of mixed phases of TiO₂.

References

- [1] M. Z. Atashbar, H. T. Sun, B. Gong, W. Wlodarski, R. Lamb, Thin Solid Films 326, (1998) 238.
- [2] T. Takeuchi, Sens Actuators, 14, (1988) 109.
- [3] W. Gopel, G. Roker, R. Feierabend, Phys. Rev B 28(6), (1993) 3427.
- [4] Cheol Ho Heo, Soon-Bo Lee, Jin-Hyo Boo, Thin Solid Films, 475, (2005) 183.

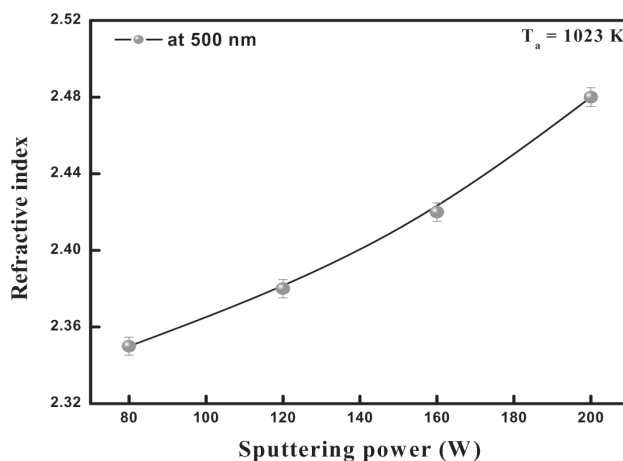


Fig.3.4: Variation of refractive index with sputter power of TiO₂ films

- [5] R. Wang, K. Hashimoto, A. Fujishima, M. Chikuni, E. Kojima, A. Kitamura, M. Shimohigoshi and T. Watanabe, Nature, 388 (1997) 431.
- [6] T. Watanabe, A. Nakajima, R. Wang, M. Minabe, S. Koizumi, A. Fujishima and K. Hashimoto, Thin Solid Films, 351 (1999) 260.
- [7] K. Takagi, T. Makimoto, H. Hiraiwa and T. Negishi, J. Vac. Sci. Technol., A 19(6) (2001) 2931.
- [8] S. Ben Amor, G. Baud, J. P. Besse and M. Jacquet, Materials Science and Engineering, B47 (1997) 110.
- [9] J. Szczyrbowski, G. Bräuer, M. Ruske, J. Bartella, J. Schroeder and A. Zmelty, Surface and Coatings Technology, 112 (1999) 261.
- [10] N. Martin, C. Rousselot, D. Rondot, F. Palmino and R. Mercier, Thin Solid Films, 300 (1997) 113.
- [11] M. Takeuchi, N. Yamasaki, K. Tsujimaru, Chem. Lett., 35 (2006) 904.
- [12] A. Verma, A.G. Joshi, A.K. Bakshi, S.M. Shivaprasad and S.A. Agnihotry, Appl. Surf. Sci., 252 (2006) 5131.
- [13] I. Turkevych, Y. Pihosh, M. Goto, A. Kasahara, M. Tosa, S. Kato, K. Takehana, T. Takamasu, G. Kido and N. Koguchi, Thin Solid Films, 516 (2007) 2387.
- [14] M. Vishwas, S.K. Sharma, K. Narshimha Rao, S. Mohan, K.V.A. Gowda and R.P.S. Chakradhar, Spectrochim. Acta, Part A 74 (2009) 839.
- [15] X. Wang, H. Masumoto, Y. Someno and T. Hirai, Appl. Phys. Lett., 72 (1998) 3264.
- [16] P. Lobl, M. Huppertz and D. Mergel, Thin Solid Films, 251 (1994) 72.
- [17] T. Asanuma, T. Matsutani, C. Liu, T. Mihara and M. Kiuchi, J. Appl. Phys., 95 (2004) 6011.
- [18] JCPDS, International Center for Diffraction Data, card No. 084-285.
- [19] G. He, Q. Fang, L. Zhu, M. Liu and L. Zhang, Chem. Phys. Lett., 395 (2004) 259.
- [20] K.F. Albertin and I. Pereyra, Thin Solid Films, 517 (2009) 4548.
- [21] S. Duenas, H. Castan, H. Garc a, E. San Andres, M.T. Luque, I. Martil, G.G. D az, K. Kukli, T. Uustare and J. Aarik, Semicond. Sci. Technol., 20(2005) 1044.
- [22] R. Swanepoel, J. Phys. E: Sci. Instrum., 16 (1983) 1214.

Formulation and Evaluation of Sustained Release Matrix Tablet

Y.NAGA LAXMI¹, P.AMARESHWAR², S.MAANASA³, M.V.RAMANA⁴, AND P.SRAVANTHI⁵

¹⁻⁵Department of Pharmaceutics

²Professor at University College of Technology

^{4,5}Associate Proffesor and Assistant professor at GBN Institute of pharmacy,
EduLabad, Ghatkesar, R.R.Dist.,Andhra Pradesh.

ABSTRACT

The main objective of the study was to develop an oral sustained release Matrix Tablets of Ciprofloxacin hydrochloride using natural Tamarind seed polysaccharide Tsp (T1-T6) and synthetic Poly methyl methacrylate PMMA (P1-P6) and combination of Tsp and synthetic PMMA (C1-C6) with various concentrations by direct compression method. The Tsp was extracted from tamarind kernel powder, it is a hydrophilic and rate controlling polymer. The prepared pre-compression blend was evaluated for pre-compression tests and post-compression tests. All the formulations showed compliance with pharmacopeia standards. The in vitro release study of matrix tablets was carried out in phosphate buffer pH 6.8 for 12 hr. Among the formulations (T1-T6), T4 with 20%TSP showed 98.64% for 12 hrs., (P1-P6), P3 with 15% of PMMA showed 96.52% for 12 hrs, (C1-C6) C4 formulation with (15% PMMA & 5%TSP) showed 98.47% for 15 hrs. The results indicated that all the above three types of formulations have shown sustained release action initially from 5hrs of pure drug to 15hrs and further, hence the objective of the study has been achieved. The release data was fitted to various mathematical models such as, Higuchi, Korsmeyer-Peppas, First-order, and Zero order to evaluate the kinetics and mechanism of the drug release. All the formulations follow zero order kinetics and the mechanism of the drug release through non-Fickian diffusion.

Key-words: Tamarind seed polysaccharide (TSP), Polymethylmethacrylate (PMMA), Ciprofloxacin hydrochloride, Matrix tablets.

Introduction

Oral route has been the commonly adopted and most convenient route for the drug delivery.

Among various dosage forms, matrix tablets are widely accepted for oral controlled release as they are simple to formulate and easy to produce. Polymers and release retarding materials used as matrix play a vital role in controlling the drug release from matrix tablets. Ideal, oral CR systems are reliant upon the dosage form to control the rate of drug release with little or no effect from the intrinsic properties of the drug¹.

Though a variety of substances are available to serve as release retarding materials for matrix tablets. The various polysaccharides used in drug delivery application are cellulose ethers, xanthan gum, locust bean gum and guar gum. Another natural polysaccharide, Tamarind seed polysaccharide (TSP) obtained from the seed kernel of *Tamarindus indica*², possesses properties like high viscosity³,

broad pH tolerance, noncarcinogenicity, mucoadhesive nature, and biocompatibility. It is used as stabilizer, thickener, gelling agent, and binder in food and pharmaceutical industries. Hydrophilic polymers when in contact with water; they are hydrated to form a gel. Because of this property natural gums have been reported as good matrix materials for sustained release matrix tablets.

Ciprofloxacin comes under the category of Fluorinated 4-quinolones. It has a broad antimicrobial activity and is effective after oral administration for the treatment of a wide variety of infectious diseases. The aim of the study was to formulate and evaluate ciprofloxacin hydrochloride sustained release matrix tablets.

Materials and Methods

Ciprofloxacin Hydrochloride was obtained as gift sample from Suzikem Drugs Pvt. Ltd. Tamarind Seeds were obtained from market, Polymethylmethacrylate was purchased from LG MMA CORP. Lactose, Magnesium stearate, and Talc was of S.D. Fine Chemicals.

*Address for correspondence: ynaga9999@gmail.com

Isolation of TSP

The tamarind seeds were dried in a hot oven at 100°C for 30 min and the seed coat was manually removed from the seeds. Then, they were milled and ground through a 45mesh sieve.

TSP was isolated following the method reported by Rao et al (1973). To 20g of tamarind kernel powder, 200ml of cold distilled water was added and slurry was prepared. The slurry was poured into 800ml of boiling distilled water. The solution was boiled for 20 minutes under stirring condition in a water bath. The resulting thin clear solution was kept overnight so that most of the proteins and fibers settled out. The solution was then centrifuged at 5000 rpm for 20 minutes. The supernatant was separated and poured into twice the volume of absolute ethanol by continuous stirring. The product was filtered through muslin cloth and was pressed between felt. The precipitate was washed with absolute ethanol, iso-propanol and methanol and then dried. The dried material was ground and sieved to obtain granules of different particle size range and stored in a desiccator until further use.

Formulation of Tablets Eighteen different formulations of matrix tablets containing ciprofloxacin hydrochloride and other additives were prepared by direct compression the concentration of the drug was kept at 50% weight of the tablet (500mg/tablet) TSP, PMMA in different proportions were used as polymers. Varying proportions of lactose was used as diluents. To prepare the tablets, the ingredients were weighed accurately and were screened through #60 mesh sieve. All ingredients except lubricant were then combined and passed through #60 mesh sieves, following the addition of the given amount of lubricant and further mixing, the powder was passed through #60 mesh sieves. The blend was compressed into tablets weighing 1000mg using rotary tablet compression machine equipped with 14mm flat punch. The tablets formulation (T1-T6), containing tamarind seed polysaccharide in different concentrations 5-30%, (P1-P6) containing polymethyl-methacrylate in different concentrations 5-30%, (C1-C6) containing combination of TSP&PMMA with different amount of lactose were prepared according to the composition in Table 1. All the preparations were stored in airtight containers at room temperature for further evaluation.

Preformulation studies

The ciprofloxacin hydrochloride tablets were determined by the parameters like identification of pure drug by IR spectra, solubility, drug excipients, compatibility studies, angle of repose, bulk density, tapped density, Hausner ratio, Carr's index were evaluated.

Evaluation Parameters

The properties of the matrix tablet, such as hardness, friability, weight variation, drug content and swelling index

were determined standard procedures. Briefly, hardness was determined using Monsanto hardness tester. Friability was determined by using Roche friability testing apparatus. Weight variation and drug content were performed according to IP procedures.

Ten tablets were weighed and average weight is calculated. All the ten tablets were crushed in a mortar. Powder equivalent to 500mg of ciprofloxacin hydrochloride was dissolved in 250 ml distilled water and was shaken for 20 mins. Solution was filtered and 5 ml filtrate was diluted to the 100ml using distilled water. Absorbance of resultant solution was measured at 278 nm using distilled water as blank. Amount of drug present in one tablet was calculated.

Swelling Studies

The extent of swelling was measured in terms of % weight gain by the tablet. The swelling behavior of all formulations was studied. One tablet from each formulation was kept in a petri dish containing pH 6.8 phosphate buffers. At the end of 1 h, the tablet was withdrawn, soaked with tissue paper, and weighed. The weights of the tablets were noted, and the process was continued till the end of 10 h. Percent weight gained by the tablet was calculated by formula. The extent of swelling was measured in terms of % weight gain by the tablet.

$$S.I = \{(M_t - M_0) / M_0\} \times 100$$

S.I = swelling index, M_t = weight of tablet at time's' & M_0 = weight of tablet at time $t = 0$.

In-vitro drug release studies

Dissolution of the tablet of each batch was carried out using USP type II apparatus using paddle. The dissolution medium consisted nine hundred ml of phosphate buffer pH 6.8 from 1 to 12 hours, maintained at 37 ± 0.5 °C. One tablet was placed in each dissolution vessel and the paddle rotational speed was set at 50 rpm. 5 ml of sample was withdrawn at every hour for 24 hours and same volume of fresh medium was replaced every time. The samples were analyzed for drug content at wavelength of 278 nm using double beam UV visible spectrophotometer. The content of drug was calculated using the equation generated from standard curve. The % cumulative drug release was calculated.

Kinetic Treatment of Dissolution Data: To describe the drug release characteristic from the prepared matrix tablets, the in-vitro dissolution data obtained was fitted to different kinetic models like; Zero order, First order, Higuchi, Peppas results are shown in respective tables.

Results and Discussion

Sustained release matrix tablets of ciprofloxacin hydrochloride were formulated and evaluated using natural hydrophilic Tamarind seed polysaccharide (T1-T6) and hydrophobic polymethylmethacrylate (P1-P6) and

combination of tamarind seed polysaccharide and polymethylmethacrylate(C1-C6) by direct compression method. Preformulation studies like physical characteristics, compatibility studies, solubility, and flow properties were performed. There was no compatibility between the pure drug, TSP and PMMA. Flow properties for isolated tamarind seed polysaccharide are presented in table no.2. All the parameters have been found to be within specified limits.

Physical properties for pre compression blend were performed for all batches shown in table no:3 that all batches had fair flow properties.

The prepared matrix tablets of all formulations were about white in colour, circular in shapes with smooth surface. All the formulations were evaluated for hardness, friability, weight variation, drug content, thickness, and swelling index. As summarized in Table no.4 for all formulations & were found to be within IP limits.

The swelling index for formulations T1-T6 was shown in fig.1 as the time increases the swelling index was increased, because weight gained by tablet was increased proportionally with the rate of hydration upto 10 hrs. Later on it may decrease gradually due to dissolution of outer most gelled layer of tablet into dissolution medium. The direct relationship was observed between swelling index and polymer concentration, as the polymer concentration increases, swelling index was increased.

The swelling index for formulations P1-P6 was shown in fig.2. As the polymer concentration increased % of swelling index was increased.

The in-vitro drug release of the matrix tablets of formulations T1-T6 were shown in fig.3 T1 formulation showed drug release 99.71% for 6hrs, T2 showed 100.82% for 7hrs, T3 showed 98.12% for 9hrs, T4 showed 98.64% for 12hrs, this is mainly due to increasing polymer concentration, also the percentage of diluents increased, the drug release also maximum because the diluent lactose is water soluble would undergo dissolution and that may result in reduction in the tortuosity and gel strength of the polymer⁴.

The drug release from the formulations T5 and T6 showed 79.11%, 68.79% respectively, It has been observed that the cumulative percentage of drug release decreasing with increasing concentration of TSP polymer and swelling index. The reason attributed to this fact is slow erosion of the gelled layer from the tablets containing higher amount of TSP. This slow release is because of the formation of a thick gel structure that delays drug release from tablet matrix, where hydration of individual TSP particles results in extensive swelling. As a result of rheology of hydrated product, the swollen particles coalesce. This results in a continuous viscoelastic matrix that fills the interstices,

maintaining the integrity of the tablet, and retarding further penetration of the dissolution medium. From all formulations T4 with 200mg showed % of drug release with maximum sustained release action. Hence formulation T4 was selected as optimized formulation.

The in-vitro drug release of the matrix tablets of formulations P1-P6 were shown in fig. 4. The increase in concentration of PMMA resulted in decrease of the drug release rate which may be due to the possible changes in the porosity and tortuosity of the matrix. From the formulation P1, P2, P3, drug release rate was up to 99.61%, 98.65%, 96.5% for more than 6, 8, 12hrs is due to increase in lactose concentration, which may be due to higher solubility of lactose, which dissolves and increases the number of pores in the matrix, making the dissolution medium penetrable. Thus lactose comes in contact with the drug in the matrix which dissolves in it and then diffuses out through the pores⁵. From the formulation P4, P5, P6, drug release rate was up to 85.62%, 74.21%, 62.52% for more than 10, 10, 9 hrs. It has been observed that the cumulative percentage of drug release was decreasing with increasing concentration of PMMA. The reason attributed to this fact is the formation of a thick layer of PMMA over the tablet due to increase in the concentration after the optimum concentration. This results in delay of drug release from tablet matrix and retarding further penetration of the dissolution medium. From the above results it was found that the formulation P3 showed sustained drug released for 12hrs.

The in-vitro drug release of the matrix tablets of formulations C1-C6 were shown in fig.5. From the formulations C1, C2, C3 with 5% of PMMA and varying concentration of TSP (5%, 10%, 15%) showed drug release 99.54 % for 10hrs, C2 96.7% for 12hrs, C3 89.7% for 14hrs with increased concentration of TSP it is showing prolonged release but release rate was decreased by forming a thick gel layer around the tablet.

C4, C5 with 5% TSP and varying concentration of PMMA (10%, 15%) showed drug release for 98.47% for 15hrs, 87.91% for 14hrs. Increased concentration of PMMA showed thick viscous layer around the tablet. C6 with 10% of TSP and 10% of PMMA showed drug release 81.16% for 11hrs.

The formulation C4 was found to be an optimum concentration for sustaining the drug release of 99.54% for 15hrs, the reason attributed was increase in concentration of lactose increases the release rate as it dissolves and increases the number of pores in the matrix, making the dissolution medium more penetrable. Thus lactose comes in contact with the drug in the matrix which dissolves in it and then diffuses out through the pores. Consequently, the formulation C4 was found to be optimized formulation containing a combination of Hydrophilic polymer PMMA (10%) and Hydrophilic polymer TSP (5%).

The kinetic treatment reflected that release data of Tsp that is T1-T6, P1-P6 and C1-C6 fig.6-11 (First order kinetics & Korsmeyer-peppas) showed higher R^2 value i.e. (0.9151 to 0.9772) for first order plot indicating that release of drug follows first order kinetics, further korsmeyer and peppas equation resulted into value of n in the range of

0.347-0.497 with all tablets indicating that the dominant mechanism of drug release through all types of matrices was by **swelling** and **erosion** which is always associated with diffusion mechanism. It can be non-fickian diffusion mechanism.

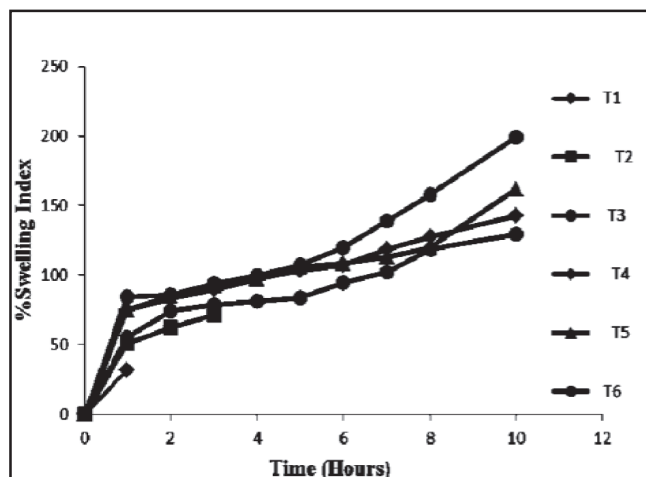


Fig.1 : % Swelling Index T1-T6

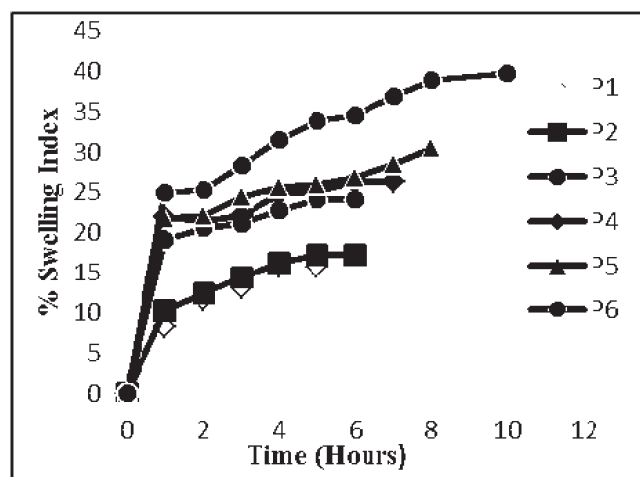


Fig. 2 : % Swelling Index P1-P6

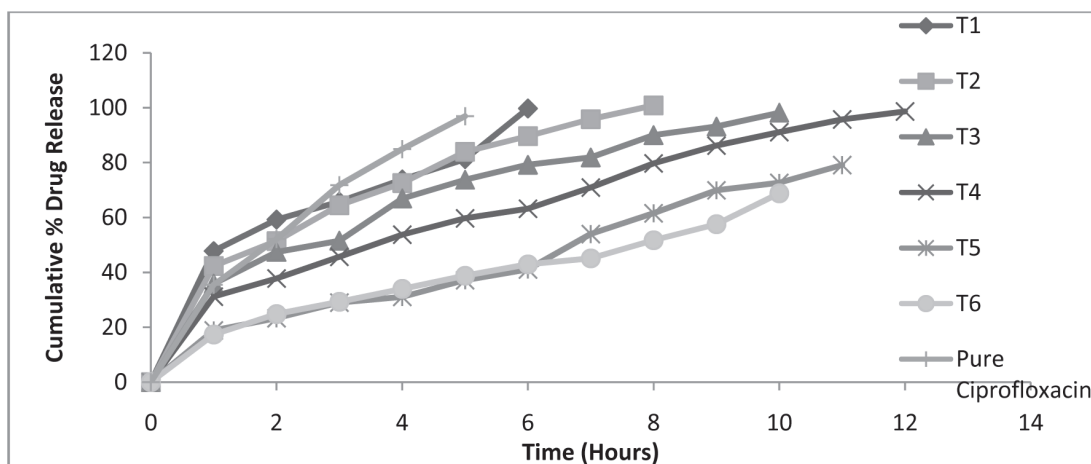


Fig.3 : Cumulative % Drug Release from (T1-T6)

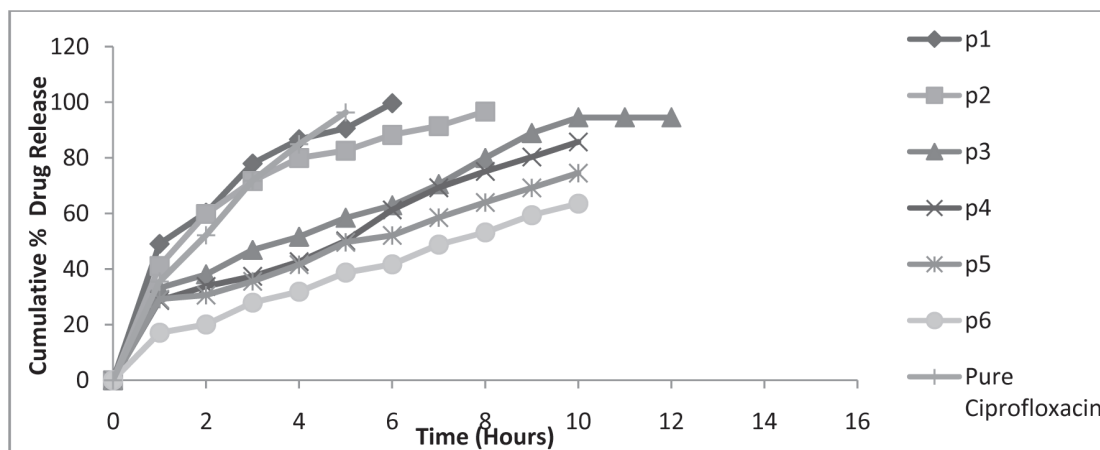


Fig. 4 : Cumulative % Drug Release from (P1-P6)

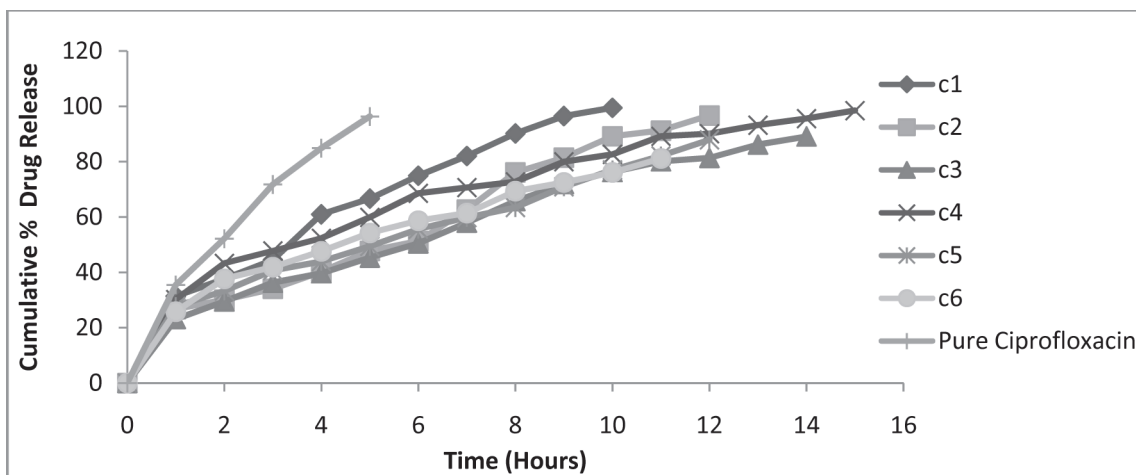


Fig. 5 : Cumulative % Drug Release from (C1-C6)

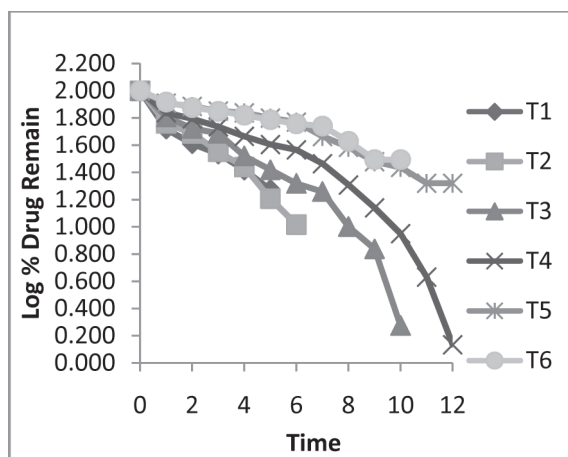


Fig. 6 : First Order Kinetics plots for T1-T6

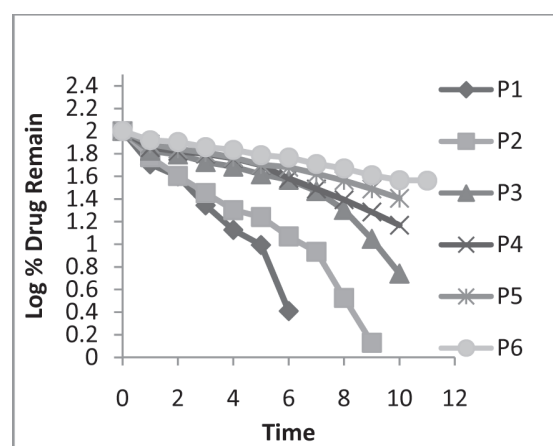


Fig. 7 : First-order plots for T1-T6

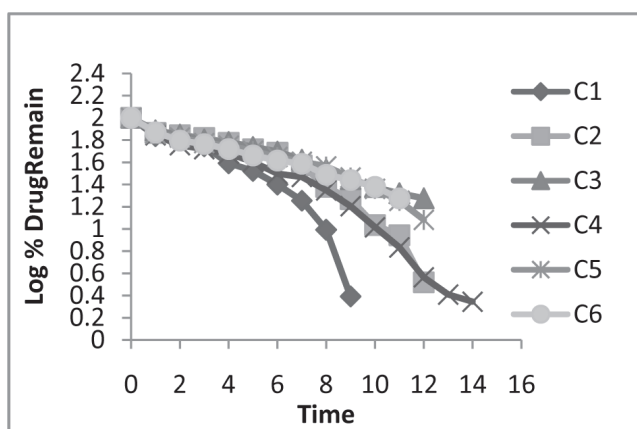


Fig. 8 : First-order plots for P1-P6

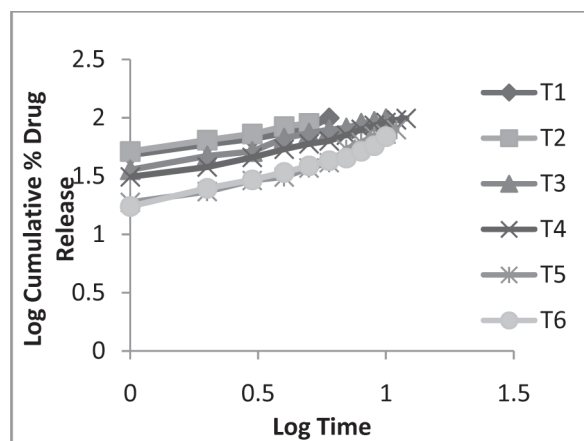


Fig.9 : Korsemeier- Peppas plot for T1-T6

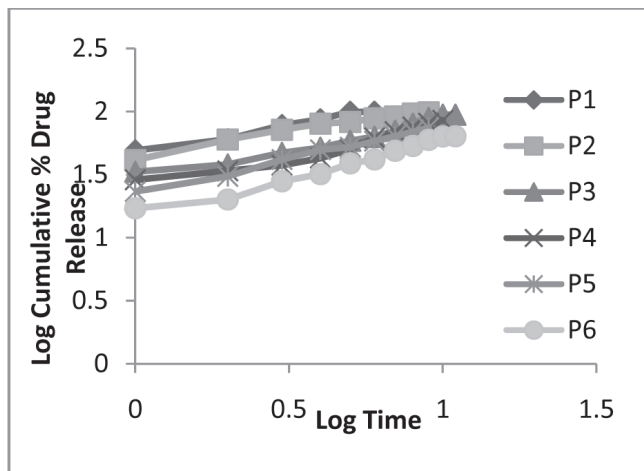


Fig.10 : Korsemeyer- Peppas plots for P1-P6

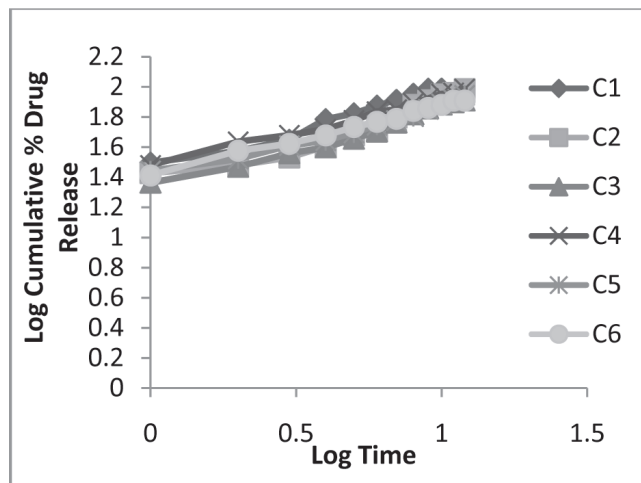


Fig. 11 : Korsemeyer- Peppas plot for C1-C6

Table - 1
Formulation Table

Formulation Code	Drug (%)	TSP (%)	PMMA (%)	Lactose (%)	Magnesium stearate (%)	Talc (%)
T1	50	5	-	40	4	1
T2	50	10	-	35	4	1
T3	50	15	-	30	4	1
T4	50	20	-	25	4	1
T5	50	25	-	20	4	1
T6	50	30	-	15	4	1
P1	50	-	5	40	4	1
P2	50	-	10	35	4	1
P3	50	-	15	30	4	1
P4	50	-	20	25	4	1
P5	50	-	25	20	4	1
P6	50	-	30	15	4	1
C1	50	5	5	35	4	1
C2	50	10	5	30	4	1
C3	50	15	5	25	4	1
C4	50	5	10	30	4	1
C5	50	5	15	25	4	1
C6	50	10	10	25	4	1

Table - 2 : Physical Properties of (TSP)

Property	Results
Bulk Density	0.4±0.009g/cc
Tapped Density	0.55± 0.005 g/cc
Compressibility Index	21.273±0.88 %
Hausner's Ratio	0.375±0.022
Angle of repose(θ)	27.203±0.010°
Swelling Index	88.8 %
pH	6.5

Table - 3
Physical Properties of Pre-Compression

Formulation code	Bulk Density (g/cc)	Tapped Density (g/cc)	Compressibility Index (%)	Hausners Ratio	Angle of Repose
T1	0.381±0.004	0.412±0.006	14.61± 1.58	1.088±0.02	28.311±0.010
T2	0.373±0.006	0.452±0.005	13.29±0.88	1.150±0.04	26.69±0.022
T3	0.312±0.004	0.358±0.002	12.84±1.11	1.150±0.04	26.12±0.066
T4	0.346±0.004	0.404±0.006	14.35±1.48	1.160±0.01	26.0±0.044
T5	0.307±0.006	0.444±0.004	13.46±1.07	1.162±0.04	26.05±0.028
T6	0.384±0.004	0.441± 0.006	13.46±1.68	1.153±0.01	25.98±0.011
P1	0.356±0.002	0.407±0.002	14.18±0.88	1.16±0.02	28.31±0.05
P2	0.354±0.006	0.398±0.006	11.55±1.48	1.16±0.09	28.38±0.07
P3	0.348±0.004	0.407±0.006	14.12±1.55	1.17±0.02	28.38±0.07
P4	0.342±0.002	0.399±0.004	14.28±1.48	1.17±0.02	28.36±0.06
P5	0.361±0.004	0.395±0.002	14.92±1.71	1.12±0.06	28.36±0.06
P6	0.333±0.006	0.407±0.004	14.28±1.42	1.17±0.02	28.24±0.01
C1	0.381±0.004	0.412±0.006	14.61± 1.58	1.088±0.02	28.31±0.010
C2	0.373±0.006	0.452±0.005	13.29±0.88	1.150±0.04	26.69±0.022
C3	0.312±0.004	0.358±0.002	12.84±1.11	1.152±0.02	26.12±0.066
C4	0.346±0.004	0.404±0.006	14.35±1.48	1.160±0.01	26.02±0.044
C5	0.307±0.006	0.444±0.004	13.46±1.07	1.162±0.04	26.05±0.028
C6	0.384±0.004	0.441±0.006	13.46±1.68	1.153±0.01	25.98±0.011

Table - 4
Physical Properties of Matrix Tablets

Formulation code	Hardness (kg/cm ²)	Friability (%)	Weight variation (mg)	Drug Content (%)	Thickness (mm)
T1	6.92±0.25	0.53±0.090	995.6±0.78	98.19±0.04	4.45±0.18
T2	7.01±0.21	0.49±0.044	992.1±0.62	99.34±0.34	4.44±0.22
T3	6.22±0.10	0.47±0.086	995.8± 0.68	92.42±0.80	4.42±0.16
T4	7.88±0.18	0.51±0.027	993.2± 0.41	99.29±0.88	4.99±0.21
T5	7.38±0.11	0.55±0.020	991.85±0.68	98.18±0.64	4.46±0.16
T6	7.15±0.21	0.50±0.038	998.6± 0.52	96.47±0.42	4.49±0.20
P1	6.82±0.24	0.47±0.33	999.3±0.967	92.18±0.98	4.45±0.28
P2	6.38±0.18	0.41±0.065	995.6±0.78	91.45±0.77	4.42±0.22
P3	6.50±0.16	0.46±0.019	993.2± 0.41	93.47±0.66	4.48±0.19
P4	6.75±0.10	0.43±0.042	992.1±0.62	95.68±0.32	4.49±0.10
P5	6.19±0.05	0.43±0.049	995.6±0.78	95.39±0.28	4.46±0.16
P6	7.34±0.09	0.50±0.04	998.6± 0.52	99.29±0.18	4.48±0.05
C1	7.15±0.21	0.52±0.018	998.6± 0.52	98.34±0.72	4.47±0.18
C2	7.72±0.12	0.54±0.043	993.2± 0.41	94.64±0.46	4.41±0.05
C3	7.22±0.10	0.51±0.018	999.7± 0.22	95.32±0.51	4.49±0.17
C4	7.58±0.16	0.54±0.052	998.6± 0.52	92.73±0.83	4.45±0.22
C5	7.97±0.24	0.55±0.092	991.85±0.68	98.56±0.53	4.49±0.26
C6	6.68±0.12	0.51±0.082	995.6±0.78	93.56±0.41	4.48±0.24

Conclusion

The study was undertaken with an aim to formulation and evaluation of sustained release matrix tablets using various polymers like TSP, PMMA. The formulations were to in-vitro release studies showed the following results; Natural polymer TSP with 20% could release the ciprofloxacin hydrochloride effectively for 12hrs. Synthetic polymer PMMA with 15% could release the ciprofloxacin hydrochloride effectively for 12hrs. Matrix tablet prepared with 150mg PMMA & 50mg TSP showed 98.47% at the end of 15hrs and it is far better system for once-daily sustained release of highly water soluble drug like ciprofloxacin hydrochloride. All the formulations were all subjected to model fitting analysis to know the order and mechanism of drug release. The data clearly shows that, the release kinetics reveals that all the formulation follows first order kinetics with non-fickian diffusion mechanism.

References

- [1] KD Tripathi. Essentials of Medical Pharmacology, Jaypee Brothers, 4th ed. Delhi; 1996,
- [2] ArkhelAlka. Formulation development and evaluation of sustained release matrix tablet of lamivudine using tamarind seed polysaccharide. *Scholars Research Library*, [Online]. 2011, 3(4), 20-28.
- [3] Yokko Nitta, 2005. Gellation and gel properties of polysaccharides gellam gum and tamarind xyloglucan. 47-52.
- [4] RishabhaMalviya, 2010. Formulation, Evaluation and Comparison of Sustained Release Matrix Tablets of Diclofenac Sodium Using Natural Polymers as Release Modifier, 12.
- [5] Çapan.Y. Formulation and Invitro - Invivo Evaluations on Sustained Release Acetylsalicylic Acid Tablets. 1989.



Formulation and Evaluation of Fast Dissolving Tablets of Poorly Water Soluble Drug

S. MAANASA¹, P. AMARESHWAR², Y. NAGA LAXMI³, M.V. RAMANA⁴, AND P. SRAVANTHI⁵

¹⁻⁵Department of Pharmaceutics

²Professor at University College of Technology, Osmania University

^{4,5}Associate professor and Assistant professor at GBN Institute of pharmacy
Edulabad, Ghatkesar-501301, R.R.Dist., Andhra Pradesh.

ABSTRACT

The aim of the study was to enhance the solubility of a drug with poor water solubility using PolyEthyleneGlycol-6000 as carrier. The Solid dispersions were prepared by Physical mixture method, by varying the drug:carrier ratio from 1:1 to 1:6. The solubility of drug was found to be enhanced by the solid dispersion technique. In order to further enhance the solubility, different combinations of superdisintegrants were used. The Fast dissolving tablets were prepared by Direct compression method with three different combinations of superdisintegrants Croscarmellose, Sodium starch glycolate (A1 to A6); Crospovidone, Sodium starch glycolate (B1 to B6); Crospovidone, Croscarmellose, Sodium starch glycolate (C1 to C6). The in-vitro drug release studies of the above formulations showed further increase in the solubility of drug. The optimized formulation C5 (1:5) showed a release of 99.05% within 30 min. The dissolution profile data was fitted to various mathematical models such as First-order and Zero order to evaluate the kinetics of the drug release. All the formulations followed first order kinetics.

Key-words: Solid dispersions, PolyEthylene Glycol-6000, Superdisintegrants, Fast dissolving tablets.

Introduction

The solubility behavior of a drug is the key determinant of its oral bioavailability. There are always certain drugs for which solubility has presented a challenge to the development of a suitable formulation for oral administration. In case of poorly water soluble drugs, dissolution rate is the rate limiting step in process of drug absorption which is a potential bioavailability problem. An estimate reports that currently about 40% of marketed Immediate Release (IR) Oral drugs are categorized as practically insoluble (100mg/mL). Although most of the drugs have encouraging experimental data obtained in-vitro, the in-vivo but results have been disappointing.

The attributes include:

- 1) Poor absorption, rapid degradation resulting in insufficient concentration
- 2) Drug distribution to other tissues with high drug toxicities
- 3) Poor solubility of drugs

The most attractive option for increasing the release rate is improvement of the solubility through formulation approaches. There are drug candidates that have poor water solubility in water but can be dissolved by suitable conventional formulation strategies such as Co-solvents, Milling techniques, super critical processing, solid dispersions including Complexation and precipitation techniques. Solid dispersion technique has often proved to be the most commonly used in improving dissolution and bioavailability of poorly water soluble API because it is simple, economic and advantageous. In solid dispersion technique, water soluble carriers are used to improve dissolution characteristics of poorly water soluble drugs. Several new technologies are available to improve the patient compliance. Fast dissolving drug delivery system (FDSD) is gaining popularity as they do not cause any obstacle in swallowing^[1].

USFDA defined FDTs as “A solid dosage form containing medicinal substances which disintegrate rapidly within few seconds to three minutes when placed up on tongue”.

*Address for correspondence:
smaanasa21@gmail.com

Advantages of Formulating the Fast dissolving tablets^[2]

- Do not require water to swallow and will dissolve or disintegrate in the mouth within a few seconds to 3 minutes itself.
- Allow high drug loading.
- Are compatible with taste masking and other excipients.
- Leave minimal or no residue in the mouth after oral administration.
- Exhibit low sensitivity to environmental conditions such as humidity and temperature.

Materials and Methods

Materials

Table - 1

Formulation table of Solid dispersions

Sl. No.	Formulation Code	Ratio of Drug : PEG 6000	Amount of PEG6000 (mg)
1	SD 1	1:1	25
2	SD 2	1:2	50
3	SD 3	1:3	75
4	SD 4	1:4	100
5	SD 5	1:5	125
6	SD 6	1:6	150

Indomethacin was obtained as a gift sample from Super Pharma Products, Ujjain; Croscarmellose sodium, Crospovidone, Sodium starch glycolate are from Vijlak Pharma Limited, Hyderabad; PEG-6000, Magnesium stearate, Talc of SD Fine chemicals, Mumbai.

Method

Preparation of Solid Dispersion by Physical Mixture Method^[3]:

The drug was uniformly mixed with of PEG-6000 by varying the drug:carrier ratio from 1:1 to 1:6 separately using a mortar and pestle. The resulting mixtures were sieved through 80-mesh sieve, then kept in a dessicator over Calcium chloride at room temperature for 24 hr.

Preformulation studies

The solid dispersions SD1 to SD6 prepared were subjected to various preformulation evaluations namely Drug-excipient compatibility studies, Angle of repose, Bulk density, Tapped density, Hausner ratio and Carr's index.

Preparation of fast dissolving tablets^[6,7]

The Solid Dispersion equivalent to 25 mg of drug was taken and mixed with directly compressible diluent, different combinations of superdisintegrants (table 2) and other excipients in a poly-bag and mixed for 20 min. The prepared pre-compression blend was directly compressed using 7 mm, round-shaped flat punch in a 10 station tablet compression machine.

Table: 2

Formulation table

Formulation Code	Indomethacin Solid dispersion (%)		Cros-carmellose (%)	Cros-povidone (%)	SSG (%)	Mannitol (%)	Magnesium stearate (%)	Talc (%)
A1	1:1	20	2	-	4	72	1	1
A2	1:2	30	2	-	4	62	1	1
A3	1:3	40	2	-	4	52	1	1
A4	1:4	50	2	-	4	42	1	1
A5	1:5	60	2	-	4	32	1	1
A6	1:6	70	2	-	4	22	1	1
B1	1:1	20	-	2	4	72	1	1
B2	1:2	30	-	2	4	62	1	1
B3	1:3	40	-	2	4	52	1	1
B4	1:4	50	-	2	4	42	1	1
B5	1:5	60	-	2	4	32	1	1
B6	1:6	70	-	2	4	22	1	1
C1	1:1	20	2	2	4	70	1	1
C2	1:2	30	2	2	4	60	1	1
C3	1:3	40	2	2	4	50	1	1
C4	1:4	50	2	2	4	40	1	1
C5	1:5	60	2	2	4	30	1	1
C6	1:6	70	2	2	4	20	1	1

In Vitro Drug Release Study^[5]

In-vitro release studies were carried out using a modified USP XXIII dissolution test apparatus (USP Type II, ElectroLab). The dissolution fluid was 900 mL of phosphate buffer pH 6.8 at a speed of 50rpm at a temperature of $37 \pm 0.5^\circ\text{C}$ were used in each test. Samples of dissolution medium (5ml) were withdrawn at regular intervals of 5, 10, 15, 20, 25, 30 min and assayed by measuring absorbance at 323 nm.

Results and Discussion

The flow properties were evaluated for the Solid dispersions prepared, the results indicate that the powder blend has good flow properties (table 3).

The prepared fast dissolving tablets of all formulations were about white in colour, circular in shapes with smooth surface. All the formulations were evaluated for hardness, friability, weight variation, drug content, thickness, and wetting time (table 4).

Table 3
Pre-Compression properties of the blend

Formula	Angle of repose (θ) \pm SD, n=3	Bulk density \pm SD, n=3 (g/cm ³)	Tapped density \pm SD, n=3 (g/cm ³)	Percent Compressibility index (I) \pm SD, n=3	Hausner's ratio \pm SD, n=3
SD1	27.2 \pm 0.294	0.48 \pm 0.012	0.71 \pm 0.016	44.59 \pm 0.219	0.88 \pm 0.026
SD2	29.26 \pm 0.26	0.43 \pm 0.012	0.61 \pm 0.008	40.3 \pm 0.37	1.18 \pm 0.012
SD3	28.3 \pm 0.163	0.39 \pm 0.016	0.61 \pm 0.02	36.13 \pm 0.205	1.14 \pm 0.024
SD4	29.9 \pm 0.294	0.36 \pm 0.205	0.59 \pm 0.012	35.4 \pm 0.326	1.21 \pm 0.016
SD5	26.5 \pm 0.16	0.40 \pm 0.012	0.68 \pm 0.016	41.66 \pm 1.26	0.78 \pm 0.016
SD6	29.3 \pm 0.163	0.38 \pm 0.008	0.50 \pm 0.014	38.23 \pm 0.339	0.92 \pm 0.020

Table - 4
Post Compression Properties for formulations

Formula	Hardness \pm SD, n=3 (kg/cm ²)	Wettin time \pm SD, n=3 (sec)	Weight variation \pm SD, n=3 (mg)	Friability \pm SD, n=3 (%)	Thickness \pm SD, n=3 (mm)	Content uniformity \pm SD, n=3 (%)
A1	2.5 \pm 0.01	43 \pm 0.42	249.5 \pm 0.0	0.64 \pm 0.11	2.69 \pm 0.049	99.03 \pm 0.36
A2	2.5 \pm 0.04	40 \pm 0.37	249 \pm 0.02	0.74 \pm 0.20	2.67 \pm 0.119	96.76 \pm 0.47
A3	2.55 \pm 0.03	34 \pm 0.19	249 \pm 0.01	0.63 \pm 0.09	2.84 \pm 0.090	96.73 \pm 0.24
A4	2.58 \pm 0.02	27 \pm 0.61	251 \pm 0.03	0.65 \pm 0.12	2.91 \pm 0.085	95.7 \pm 0.38
A5	2.61 \pm 0.03	24 \pm 0.51	250 \pm 0.01	0.65 \pm 0.20	2.73 \pm 0.097	97.1 \pm 0.48
A6	2.55 \pm 0.01	22 \pm 0.32	249 \pm 0.05	0.63 \pm 0.13	2.82 \pm 0.127	98.33 \pm 0.46
B1	2.41 \pm 0.01	44 \pm 0.64	251 \pm 0.04	0.56 \pm 0.08	2.94 \pm 0.108	100.29 \pm 0.46
B2	2.6 \pm 0.04	39 \pm 0.25	249 \pm 0.06	0.7 \pm 0.18	2.68 \pm 0.081	99.43 \pm 0.77
B3	2.63 \pm 0.03	35 \pm 0.36	249 \pm 0.03	0.67 \pm 0.16	2.96 \pm 0.067	97.63 \pm 0.61
B4	2.52 \pm 0.01	26 \pm 0.17	250 \pm 0.04	0.61 \pm 0.14	2.81 \pm 0.111	95.24 \pm 0.54
B5	2.47 \pm 0.02	24 \pm 0.32	250 \pm 0.02	0.6 \pm 0.12	2.75 \pm 0.126	98.67 \pm 0.81
B6	2.7 \pm 0.01	23 \pm 0.21	250 \pm 0.03	0.72 \pm 0.09	2.87 \pm 0.167	96.17 \pm 0.34
C1	2.45 \pm 0.01	42 \pm 0.56	251 \pm 0.04	0.65 \pm 0.14	2.67 \pm 0.198	96.57 \pm 0.67
C2	2.64 \pm 0.02	38 \pm 0.34	251 \pm 0.03	0.69 \pm 0.07	2.86 \pm 0.154	98.3 \pm 0.73
C3	2.42 \pm 0.01	33 \pm 0.32	250.5 \pm 0.04	0.59 \pm 0.01	2.63 \pm 0.161	97.21 \pm 0.84
C4	2.64 \pm 0.03	26 \pm 0.71	251 \pm 0.02	0.66 \pm 0.03	2.95 \pm 0.095	99.5 \pm 0.67
C5	2.4 \pm 0.04	23 \pm 0.53	249 \pm 0.01	0.7 \pm 0.01	2.82 \pm 0.134	100.14 \pm 0.44
C6	2.53 \pm 0.03	22 \pm 0.27	249 \pm 0.01	0.72 \pm 0.02	2.91 \pm 0.089	97.67 \pm 0.37

Table 5
Disintegration time

Formulation Code	Disintegration time \pm SD, n=3 (sec)
A1	82 \pm 0.05
A2	78 \pm 0.07
A3	73 \pm 0.06
A4	69 \pm 0.02
A5	65 \pm 0.09
A6	68 \pm 0.01
Formulation Code	Disintegration time \pm SD, n=3 (sec)
B1	83 \pm 0.04
B2	81 \pm 0.06
B3	79 \pm 0.07
B4	74 \pm 0.03
B5	68 \pm 0.02
B6	70 \pm 0.02
Formulation Code	Disintegration time \pm SD, n=3 (sec)
C1	80 \pm 0.03
C2	76 \pm 0.08
C3	71 \pm 0.01
C4	67 \pm 0.04
C5	62 \pm 0.05
C6	66 \pm 0.07

FTIR Spectroscopy

The FTIR spectra of samples of indomethacin and excipients were shown in figure 1.

The pure drug showed numerous characteristic high intensity diffraction peaks demonstrating the crystalline nature of the drug. The diffused peaks in solid dispersion indicates the amorphization of drug. Characteristic peaks attributed to the functional groups present in the molecule of drug were assigned to establish the identity of the drug compared to solid dispersion^[4]

FTIR spectra of Indomethacin reported characteristic peaks of C=O scissoring, bending; C=C ring stretching; aromatic ring C-H stretching; C=C stretching; C=O stretching; -OC stretching and C-H stretching at 1454.38, 1587.47, 1587.47, 1645.33, 1691.56, 1149.61 and 2946.40 wave numbers respectively. The peak at 1548.89 which is attributed for C=O stretching disappeared in SD which indicates there might be the transformation of the drug into an amorphous state due to H-bond formation with the carrier or new bond formation. Drug-excipient interactions play a crucial role with respect to the stability and potency of the drug. FTIR techniques have been used to study the physical and chemical interaction between drug and

excipients used. In the spectra of the optimized formulation (figure 2), the peaks characteristic to the excipients were present at almost same positions, whereas indomethacin peaks were also present, but at a reduced intensity of absorption, indicating the trapping of the drug inside the carrier matrix. None of the spectra showed any peaks other than those assigned to drug and excipients, which indicates the absence of any well-defined chemical interactions. Results showed that there is no difference between the IR patterns of the optimized formulation of indomethacin SD ODT and pure drug and all the excipients are compatible with the solid dispersion complex.

Drug Release from the formulations

The pure drug Indomethacin has also been studied for *in-vitro* drug release and was found to be 21% for 40 mins as shown in figure. The water soluble carrier PEG 6000 was estimated to enhance the dissolution of drug. The solid dispersions prepared (SD1 to SD6) were subjected to *invitro* drug release to evaluate the efficiency of PEG 6000 in enhancing the dissolution, the formulation SD5 was found to be better with a release of 88.36% in 40 min as shown in fig 3.

The invitro drug release from the formulations A1 to A6 was increasing gradually with respect to time from A1

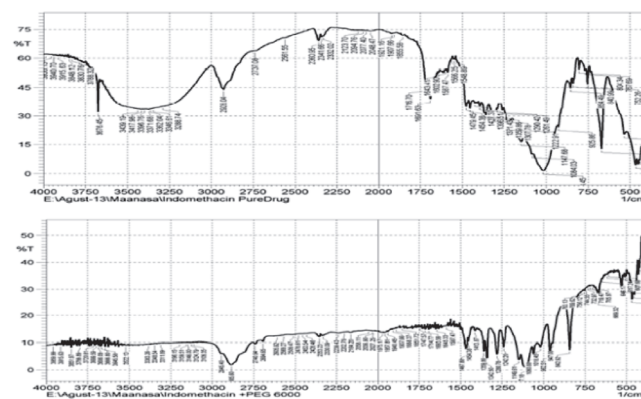


Fig. 1 : FTIR Spectra of Pure Indomethacin and Solid dispersion

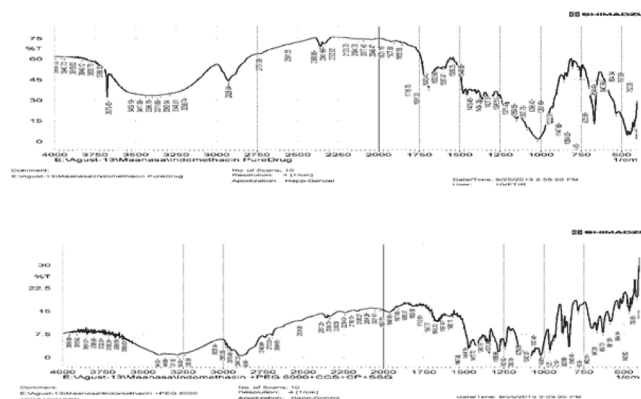


Fig. 2 : FTIR Spectra of Pure Indomethacin and Optimized formulation C5

to A5 but decreased in A6 as shown in fig 4. The drug released was found to be 98.85% for 30 min in A5. The invitro drug release in these formulations was increasing gradually with respect to time from B1 to B5 but decreased in B6 as shown in fig 5. The drug released was found to be 98.12% for 30 min in B5.

The invitro drug release in these formulations was increasing gradually with respect to time from C1 to C5 but decreased in C6. The drug released was found to be 99.05% for 30 min in C5 as shown in fig 6. The reason attributed for no further increase in A6, B6, C6 is that the carrier plasticizes and forms a thick layer decreasing the drug diffusion.

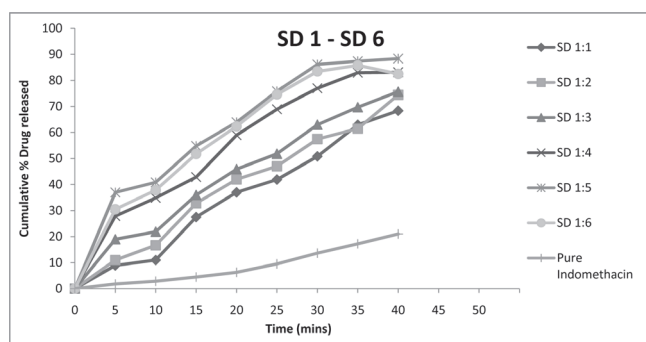


Fig. 3: Cumulative percent drug release profile Solid dispersion

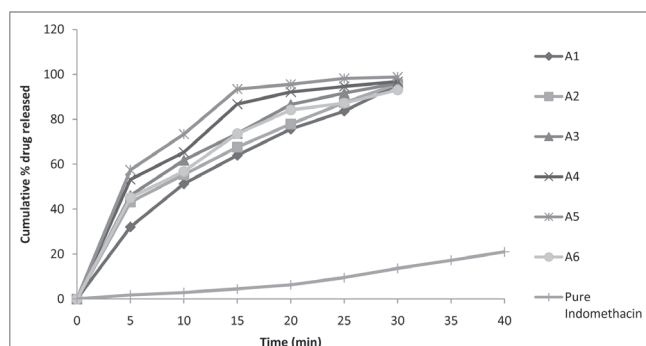


Fig. 4: Cumulative percent drug release from the formulations A1 to A6

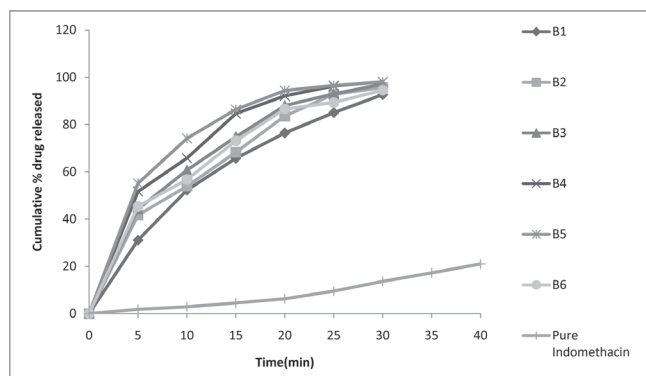


Fig. 5: Cumulative percent drug release profile of B1 to B6 formulation

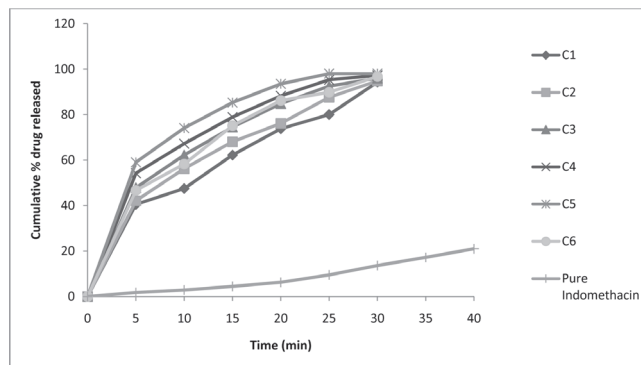


Fig. 6: Cumulative percent drug release profile of C1 to C6 formulation

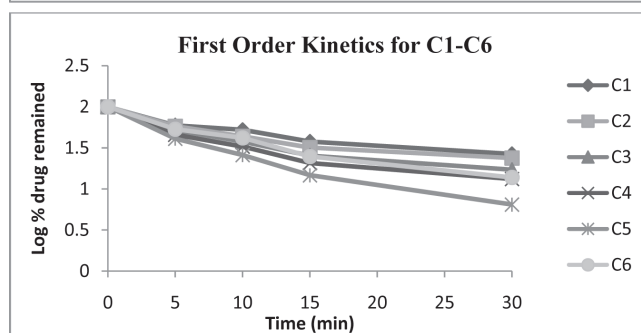
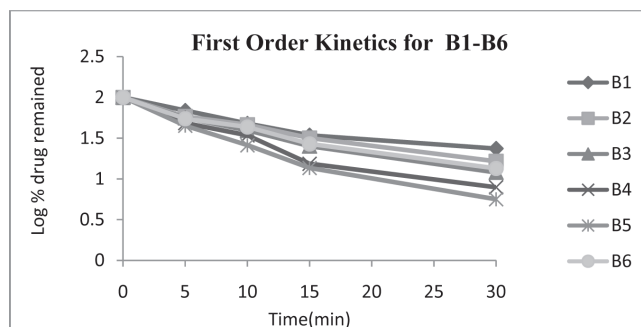
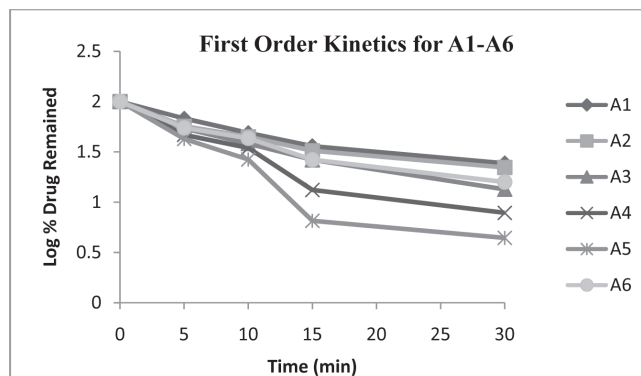


Fig. 7: First order kinetics

Effect Of PEG-6000 on the Drug Release

The In-vitro dissolution of matrix tablets of indomethacin containing hydrophilic PEG 6000 of various concentrations is studied. The drug is kept constant and the concentration of carrier was changed, the drug:carrier ratios prepared were 1:1, 1:2, 1:3, 1:4, 1:5, 1:6. SD1 formulation showed a release of 68.36%, SD2 showed a release of

74.46%, SD3 showed 75.67%, SD4 showed 83.14%, SD5 showed 88.36%, SD6 showed 82.47% in 40 min. As the PEG concentration was increased, the dissolution rate increased till SD5 but did not show any additional increase in SD6.

Increasing the PEG concentration in SD formulations only to a specific amount resulted in better drug dissolution and by further increasing the carrier concentration, it did not show any additional improvement. This might be attributed to the viscous layer formed around the solid particles due to higher PEG concentrations and therefore decreased diffusion co-efficient (based on Stokes-Einstein equation) and lower the drug dissolution. In the tablet formulations prepared with SD6, the tablets did not disintegrate in specified limit of time for fast dissolving tablet. This may be due to more hardness of the tablets as this carrier acts as strong binder at high level within the tablets.

During compression, the carrier should plastisize, soften or melt, filling the pores within tablets makes disintegration difficult, with the dissolution process of the tablet depends upon the wetting followed by disintegration of tablet.

Conclusion

The oral disintegrating tablets of indomethacin with sufficient mechanical strength, acceptable taste and smaller disintegration time were achieved employing suitable super disintegrants and other excipients at optimum concentration. The solid dispersions prepared were compressed into tablets using direct compression method by addition of superdisintegrants. The combinations of superdisintegrants were varied. The in-vitro release studies showed the following results,

- 1) Drug : Carrier ratio was varied from 1:1 to 1:6, SD5 showed the maximum release of 88.36% in 40 min.

- 2) The combination of super-disintegrants, Croscarmellose, Crospovidone and SSG was found to be more effective, showed a greater release 99.05% in 30 min.
- 3) When we compared the efficiency of the superdisintegrants combination, we found that croscarmellose,SSG which showed 98.85% in 30 min was found to be superior over crosspovidone, SSG which showed 98.12% in 30 min.
- 4) The drug release kinetics confirmed that all the formulations follow first order kinetics.

References

- 1) Gauri S, Kumar G. Fast Dissolving drug delivery and its technologies. *The PharmJ* 2011; 1(2) : 34-39.
- 2) Jagani H, Patel R, Upadhyayan P, Bhanglae J. Fast dissolving tablets : Present and future prospectus. *J Adv Pharm and health* 2011 ; 2(1) : 57-70.
- 3) Aremanda, Sindhu P. Improving solubility of poorly water soluble drug indomethacin by incorporating porous material in soli dispersion. *The Brooklyn center* 2010; 14 :110.
- 4) Sanjay Jain, 2012. Formulation and Characterization of fast disintegrating tablets containing Cefdinir solid dispersion. *International Journal of Pharmacy and Life Sciences*, 3(12), PP : 2190-2199.
- 5) Vinay Pandit, 2012. Invitro-invivo evaluation of fast dissolving tablets containing solid dispersion of Pioglitazone hydrochloride. *Journal of Advanced Pharmaceutical Technology and Research*, 3(3), PP : 160-170.
- 6) Mohd Azharuddin, 2012. Formulation and evaluation of fast dissolving tablets of Carvedilol using Sublimation technique. *International Journal of Research in BioSciences*, [Online]. 1(1), PP : 13-23.
- 7) Ganji Amarnath Reddy, 2012. Formulation and evaluation of oral fast disintegrating tablets by using Amlodipine besylate solid dispersion by Direct Compression Method. *Scholars Research Library*, 4(2), PP:683-694.



Zirconia Supported Phosphotungstic Acid Mediated Synthesis of Homoallylic Alcohols

SANNITHI SURESH BABU,* C.V. HARIHARAKRISHNA, AND K. MUKKANTI†

R. A. Chem Pharma Ltd., Prashantnagar, Kukatpally, Hyderabad-500 072. INDIA

†Center for Chemical Science and Technology, Institute of science and Technology,
JNT University Kukatpally, Hyderabad-500 085, INDIA

ABSTRACT

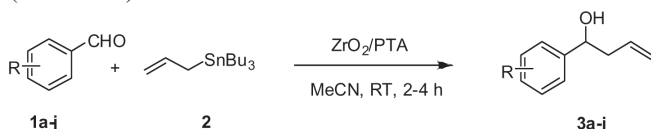
An alternative synthesis of homoallylic alcohols (**3a-j**) has been developed using zirconia supported tungstophosphoric acid (ZrO_2/PTA) as a heterogeneous catalyst with a variety of aromatic aldehydes (**1a-j**) and allyltributylstannane (**2**) at room temperature. The products were formed with in 2-5 h and good to high yields.

Key Words: Zirconia supported tungstophosphoric acid, allyltributylstannane, heterogeneous catalyst, temperature, homoallylic alcohols.

Introduction

Homoallylic alcohols¹ are important building blocks for the construction of various biologically active compounds and hence the synthesis of these compounds is highly useful. Nucleophilic addition of allyltin reagents to carbonyl compounds² in the presence of a catalyst is a straightforward method for the synthesis of homoallylic alcohols. A variety of Lewis acids (polymer-supported scandium³, ligand accelerated cadmium⁴, NbCl_5 ⁵, $\text{La}(\text{OTf})_3$ ⁶, $\text{CeCl}_3 \cdot 7\text{H}_2\text{O} \cdot \text{NaI}$ ⁷, $\text{ReBr}(\text{CO})_5$ ⁸, TCT⁹, $\text{HClO}_4 \cdot \text{SiO}_2$ ¹⁰ and potassium dodecatungstocobaltate trihydrate¹¹) including TiCl_4 , $\text{BF}_3 \cdot \text{Et}_2\text{O}$, SnCl_4 , InCl_3 , AlCl_3 and MgBr_2 . The search for new reagents capable of mediating these reactions is still a matter of much concern.

In this paper we describes our results on the use of zirconia supported tungstophosphoric acid (ZrO_2/PTA) as a heterogeneous catalyst for the synthesis of homoallylic alcohols (**3a-j**) by the reaction of a variety of aromatic aldehydes and allyltributylstannane (**2**) at room temperature (Scheme 1).



Scheme 1:
Synthesis of homoallylic alcohols

Experimental

All the commercial reagents and solvents were used without further purification unless otherwise stated. Melting points were recorded on a Buchi 535 melting point apparatus

*Address for correspondence

and are uncorrected. All the reactions were monitored by thin layer chromatography performed on precoated silica gel 60F₂₅₄ plates (Merck). Compounds were visualized with UV light at 254 nm and 365 nm, I_2 and heating plates after dipping in 2% phosphomolybdic acid in 15% aq. H_2SO_4 soln. IR spectra were recorded on a Perkin-Elmer 683 or a 1310 FT-IR spectrometers with KBr pellets. NMR spectra were recorded on a Varian Unity-400 MHz and BRUKER AMX 300 spectrometers using TMS as an internal standard. Mass spectra were recorded on a VG Micromass 7070H and a Finnigan Mat 1020B mass spectrometers operating at 70eV.

General procedure for the preparation of homoallylic alcohols: To a mixture of aldehyde (2.0 mmol) and allyltributylstannane (2.4 mmol) in acetonitrile (5 mL) ZrO_2/PTA (10 mol%) was added. The reaction mixture was stirred at room temperature and the reaction was monitored by TLC. After completion, the mixture was diluted with acetonitrile (20 mL) and filtered (to remove the catalyst). The filtrate was concentrated and gummy residue was purified by column chromatography over silica gel using 3% EtOAc in hexane to obtain following pure homoallylic alcohols:

1-Phenyl-3-buten-1-ol (3a): Pale yellow liquid, IR (neat): λ_{max} 3369, 3070, 2925, 1540, 1451, 1047, 946 cm^{-1} ; ^1H NMR (CDCl_3): δ 2.40-2.55 (m, 2H, $-\text{CH}_2-$), 4.70 (t, 1H, $-\text{CH}-$), 5.10-5.20 (dd, 2H, $=\text{CH}$), 5.70-5.85 (m, 1H, $-\text{CH}=\text{}$), 7.20-7.35 (m, 5H, Ar-H).

1-(4-Methylphenyl)-3-buten-1-ol (3b): Pale yellow liquid, IR (neat): λ_{max} 3369, 3070, 2925, 1540, 1451, 1047,

946 cm⁻¹; ¹H NMR (CDCl₃): δ 2.35 (s, 3H, -CH₃), 2.40-2.55 (m, 2H, -CH₂-), 4.70 (t, 1H, -CH-), 5.10-5.20 (dd, 2H, =CH), 5.70-5.85 (m, 1H, -CH=), 7.20-7.35 (m, 5H, Ar-H).

1-(4-Bromophenyl)-3-buten-1-ol (3c): Pale yellow liquid, IR (neat): λ_{max} 3369, 3070, 2925, 1540, 1451, 1047, 946 cm⁻¹; ¹H NMR (CDCl₃): δ 2.40-2.55 (m, 2H, -CH₂-), 4.70 (t, 1H, -CH-), 5.10-5.20 (dd, 2H, =CH), 5.70-5.85 (m, 1H, -CH=), 7.20-7.35 (m, 5H, Ar-H).

1-(4-Chlorophenyl)-3-buten-1-ol (3d): Pale yellow liquid, IR (neat): λ_{max} 3369, 3070, 2925, 1540, 1451, 1047, 946 cm⁻¹; ¹H NMR (CDCl₃): δ 2.40-2.55 (m, 2H, -CH₂-), 4.70 (t, 1H, -CH-), 5.10-5.20 (dd, 2H, =CH), 5.70-5.85 (m, 1H, -CH=), 7.20-7.35 (m, 5H, Ar-H).

1-(2,4-Dichlorophenyl)-3-buten-1-ol (3e): Pale yellow liquid, IR (neat): λ_{max} 3369, 3070, 2925, 1540, 1451, 1047, 946 cm⁻¹; ¹H NMR (CDCl₃): δ 2.40-2.55 (m, 2H, -CH₂-), 4.70 (t, 1H, -CH-), 5.10-5.20 (dd, 2H, =CH), 5.70-5.85 (m, 1H, -CH=), 7.20-7.35 (m, 5H, Ar-H).

1-(4-Methoxyphenyl)-3-buten-1-ol (3f): Pale yellow liquid, IR (neat): λ_{max} 3369, 3070, 2925, 1540, 1451, 1047, 946 cm⁻¹; ¹H NMR (CDCl₃): δ 2.40-2.55 (m, 2H, -CH₂-), 4.70 (t, 1H, -CH-), 5.10-5.20 (dd, 2H, =CH), 5.70-5.85 (m, 1H, -CH=), 7.20-7.35 (m, 5H, Ar-H).

1-(3,4,5-Trimethoxyphenyl)-3-buten-1-ol (3g): Pale yellow liquid, IR (neat): λ_{max} 3369, 3070, 2925, 1540, 1451, 1047, 946 cm⁻¹; ¹H NMR (CDCl₃): δ 2.40-2.55 (m, 2H, -CH₂-), 4.70 (t, 1H, -CH-), 5.10-5.20 (dd, 2H, =CH), 5.70-5.85 (m, 1H, -CH=), 7.20-7.35 (m, 5H, Ar-H).

1-(4-Hydroxyphenyl)-3-buten-1-ol (3h): Pale yellow liquid, IR (neat): λ_{max} 3369, 3070, 2925, 1540, 1451, 1047, 946 cm⁻¹; ¹H NMR (CDCl₃): δ 2.40-2.55 (m, 2H, -CH₂-), 4.70 (t, 1H, -CH-), 5.10-5.20 (dd, 2H, =CH), 5.70-5.85 (m, 1H, -CH=), 7.20-7.35 (m, 5H, Ar-H).

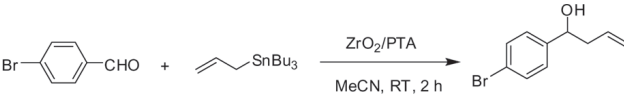
1-(4-Nitrophenyl)-3-buten-1-ol (3i): Pale yellow liquid, IR (neat): λ_{max} 3369, 3070, 2925, 1540, 1451, 1047, 946 cm⁻¹; ¹H NMR (CDCl₃): δ 2.40-2.55 (m, 2H, -CH₂-), 4.70 (t, 1H, -CH-), 5.10-5.20 (dd, 2H, =CH), 5.70-5.85 (m, 1H, -CH=), 7.20-7.35 (m, 5H, Ar-H).

1-Naphthylphenyl-3-buten-1-ol (3j): Pale yellow liquid, IR (neat): λ_{max} 3369, 3070, 2925, 1540, 1451, 1047, 946 cm⁻¹; ¹H NMR (CDCl₃): δ 2.40-2.55 (m, 2H, -CH₂-), 4.70 (t, 1H, -CH-), 5.10-5.20 (dd, 2H, =CH), 5.70-5.85 (m, 1H, -CH=), 7.20-7.35 (m, 5H, Ar-H).

Results and Discussion

Upon screening with 4-bromobenzaldehyde, it was found that ZrO₂ supported PTA with low loading (10 mol%) is an efficient catalyst to bring about this transformation at room temperature. Blank experiments have shown that the PTA alone cannot bring about this transformation. In addition, only 10 mol% ZrO₂/PTA is sufficient for the synthesis of homoallylic alcohols from the reaction of various aldehydes with allyltributylstannane. In the absence of this catalyst only a trace of amount of homoallylic alcohol could be detected even after 10 h.

Table-1
Optimizing the reaction conditions^a



Entry	Catalyst (mol%)	Time (h)	Yield (%) ^b
1	ZrO ₂ /PTA (5)	2	76
2	ZrO ₂ /PTA (10)	2	88
3	ZrO ₂ /PTA (15)	2	90
4	ZrO ₂ /PTA (20)	2	91

^a4-bromobenzaldehyde/allyltributylstannane/ZrO₂/PTA - 2:2.4:10 (mol%)

^bIsolated yields

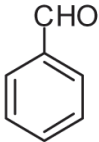
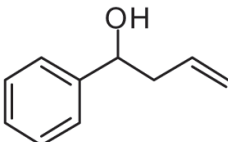
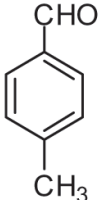
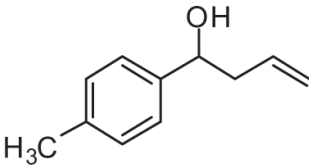
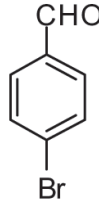
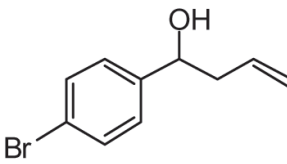
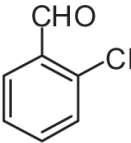
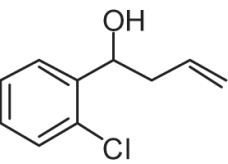
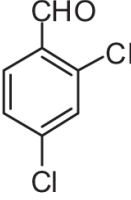
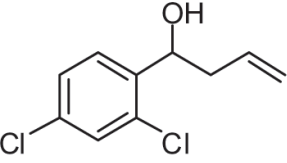
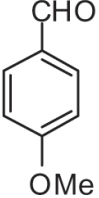
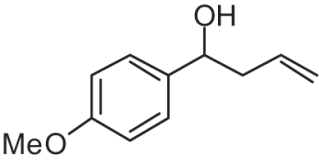
Encouraged by the results obtained from 4-bromobenzaldehyde with allyltributylstannane, we investigated a number of other aldehydes to probe their behavior under the current catalytic conditions. The aromatic aldehydes containing both electron-donating and electron-withdrawing groups in the aromatic ring proceeded smoothly.

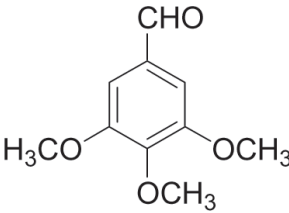
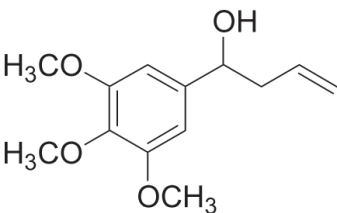
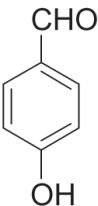
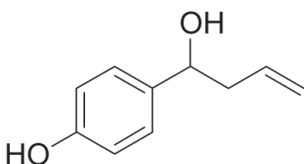
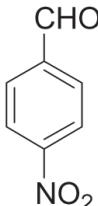
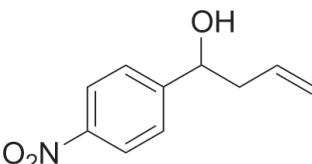
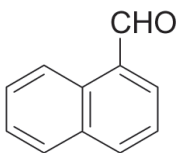
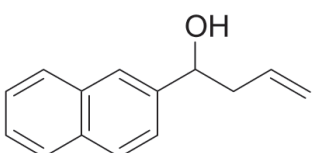
Next, we investigated the reusability and recycling of ZrO₂/PTA. At first, we put 4-bromobenzaldehyde (20 mmol), allyltributylstannane (21.6 mmol) and 100 mol% of ZrO₂/PTA in acetonitrile (50 mL) together, and then the mixture was stirred at room temperature. When the reaction was completed, the catalyst was separated by simple filtration by diluting with excess acetonitrile and recovered ZrO₂/PTA was activated and reused in subsequent reactions. Second and third reactions using recovered ZrO₂/PTA afforded similar yields to those obtained in the first run (88%). In the fourth and fifth runs, the yields were gradually decreased (80% and 75%).

Conclusions

In conclusion, we have successfully demonstrated a novel catalytic application of ZrO₂ supported phosphotungstic acid for the efficient synthesis of homoallylic alcohols. This simple procedure is efficient and can be applied to a variety of aromatic aldehydes to prepare homoallylic alcohols. The ambient reaction conditions, shorter reaction times, good to excellent product yields make this catalytic system an alternative method for the synthesis of homoallylic alcohols.

Table 2: Synthesis of homoallylic alcohols using 10 mol% of ZrO₂/PTSA

Entry	Aldehyde (1)	Product (3)	Time (h)	Yield (%)
a			2	83
b			3	85
c			2	88
d			3	80
e			3	82
f			4	85

g			2	83
h			3	85
i			2	88
j			3	80

REFERENCES

1. J.-T. Li, H.-G. Dai, W.-Z. Xu, T.-S. Li, *Ultrason. Sonochem.*, **13**, 24, (2006).
2. Z.H. Zhang, L. Yin, Y.-M. Wang, *Synthesis*, 1949 (2005).
3. S. Kobayashi, N. Aoyama, K. Manabe, *Synlett* 483 (2002).
4. H. C. Aspinall, J. S. Bissett, N. Greeves, D. Levin, *Tetrahedron Lett.*, **43**, 319 (2002).
5. G. Bartoli, M. Bosco, A. Giuliani, E. Marcantoni, *J. Org. Chem.*, **69**, 1290 (2004).
6. B. Das, K. Laxminarayana, B. Ravikanth, B. Rama Rao, *Tetrahedron Lett.*, **47**, 9103 (2006).
7. L. Nagarapu, P. Venkateswarlu, P. Gopal, unpublished work.
8. L. Nagarapu, P. Gopal, A. Satyender, *Synth. Commun.*, **39**(2), 355 (2009).



Synergistic And Individual Neurotoxicity of Fenvalerate and Azadirachtin on ATPases Activity in the Cockroach, *Periplaneta Americana*

D. ARUNA KUMARI^{1*}, K.V. MADHUSUDHAN², S. GOPAL² AND GRAJARAMI REDDY³

¹SKR and SKR Govt. Degree College (W) Kadapa, A.P, India,

²Government Degree College for Men, Kurnool, A.P, India

³Simhapuri University, Nellore, A.P, India

ABSTRACT

Synthetic Pyrethroids are widely used as insecticides because of their low application rates, rapid knockdown and low mammalian toxicity. The threat to continued use of these compounds is that of resistance in target organisms and accumulation in the environment. This consequently stimulated the search for natural compounds. Many studies revealed that the action of pyrethroids can be effectively augmented by various synergists. In this study also the efficacy of fenvalerate was increased when it was combined with azadirachtin, the most prominent phytochemical insecticide developed in recent years. The present study investigated the effect of fenvalerate, azadirachtin and synergist (a combination of both) on Adenosine Tri Phosphatases (ATPases) activity in different tissues of cockroach. Experiments were carried out using both sub lethal and lethal doses of fenvalerate, azadirachtin and synergist at 1hr, 4hr, 8hr, 12 hr and 24 hrs of post exposure. The decrease in the activity of these enzymes was in dependent manner and effect of pesticide is related to the time of exposure and its concentration. This study would contribute the useful information to the existing knowledge on the toxicity of pyrethroids, neem products and paves the way for the exploration of synergists in combination with pyrethroids and biopesticides.

Key Words: Fenvalerate, Azadirachtin, Synergist, Adenosine Tri Phosphatases, Cockroach.

Introduction

Synthetic pyrethroids are increasingly used as insecticides both in agricultural and households because of their advantageous environmental properties, short period of life, broad spectrum of insecticidal activities and low mammalian toxicity. However it has become increasingly apparent that the widespread use of synthetic pyrethroids caused detrimental environmental effects that are harmful to humans and other animals, more over target pests shown to develop resistance. This consequently stimulated the search of natural compounds that could replace the synthetic insecticides. To overcome the resistance it is common to add a synergists, mostly the botanical insecticides as they are relatively safe, degradable and readily available sources of biopesticides. Unless pyrethrins are formulated with a synergist most initially paralyzed insects recover to once again become pests (1).

Pesticides containing bioactive compounds from the neemplant, *Azadirachta indica* Juss are reported to be target specific and comparatively less toxic (2).

The potential synergistic effects of botanical seed oil *Anethem sowa* was observed on *Periplanata americana*, *Musca domestica* and *Anopheles stephensi* (3). The present work is modest attempt to know the synergist toxic effects of fenvalerate, with azadirachtin in the cockroach *Periplaneta americana*. This study would contribute useful information to the existing knowledge on the toxicity of pyrethroids and neem products and paves the way for the exploration of synergist in combination with pyrethroids and bio pesticides.

Adenosine triphosphatases ATPases are complex set of enzymes, play a central role in physiological functions of cell as energy transducers by coupling the chemical reactions(4). Mg^{2+} ATPases are mostly present in almost all cells, rich in muscle cells (5). In most cases Mg^{2+} ATPase is

*Address for correspondence:
dr.aruna_prasad@yahoo.com

taken as an index of ATPases activity because of its abundant distribution and dual localization in mitochondria and cytosol (6). $\text{Na}^+ \text{K}^+$ ATPase is present predominantly in the nerve cells (7) and is shown to be involved in the active transport of ions across the cell membrane, It is also known to associate with the uptake process of catecholamines in the central nervous system(8), Whereas Mg ATP ase is known to catalyze the terminal step of oxidative phosphorylation. In the present study also $\text{Na}^+ \text{K}^+$ ATPase was found to be high in the nervous tissue and Mg^+ ATP ase was high in muscle tissue in accordance with their functional roles in nerve conduction and muscle movements respectively. Number of studies has shown that ATPase activity was inhibited by heavy metals such as lead (9) and Cadmium (10). Inhibition of ATPases due to pyrethroids and azadirachtin were also reported (11). Since the ATPases seems to be the target enzymes for several pesticides, the activity levels of $\text{Na}^+ \text{K}^+$ ATPases, Mg^{2+} ATPases which regulate neuronal and muscular energy levels were studied in the cockroach *Periplaneta americana*.

Materials and Methods

Selection of test animals

Adult cockroaches are selected and acclimatized to the laboratory condition ($30 \pm 2^\circ\text{C}$) for one week prior to using them for the experiment. They were fed with bread and rice in a fixed time schedule. Feeding was stopped half day before the commencement of the experiments to avoid metabolic variation due to diet. Only male cockroaches were used for the study as females were known to exhibit erratic rhythmicity and influenced by the state of reproductive cycle.

Selection of test chemicals

The synthetic pyrethroid Fenvalerate 20EC and Neem derivative Azadirachtin 0.15 EC used in the present study were of commercial grade and purchased from the local market.

Preparation and application of different concentrations of chemicals

A stock solution of 20ppm of Azadirachtin and 10ppm of Fenvalerate were prepared in acetone. From this stock solution appropriate amounts were aliquot in distilled water to prepare different concentrations of chemicals. Synergist was prepared by mixing equal volumes of fenvalerate and azadirachtin. All these chemicals of different concentrations were used for topical exposure to determine LD_{50} .

Selection of chemical dose (lethal and sub lethal)

Toxic interaction of chemical with a given biological system is dose related. The 24 hr LD_{50} (dose required to kill 50% of the animals after 24hrs of exposure) was

determined using Probit method and calculated by adapting the Carpenter formula. $1/3^{\text{rd}}$ of 24 hr LD_{50} was selected as sub lethal dose. Experiments were conducted using both lethal and sub lethal doses and were carried out at 1hr, 4hr, 8hr 12hrs and 24hrs of after exposure.

Estimation of Adenosine Triphosphate (ATPase) activity (EC 3.6.1.3)

Total and Mg^{2+} ATPase activities in the tissues were estimated by the method of Tirri *et al* (12). 1% homogenates of the tissues were prepared in 0.25 M ice cold sucrose solution. Homogenates were divided into two parts. One part was centrifuged at 1400g and the supernatant thus obtained was used as an enzyme source for Mg^{2+} ATPase, while the other part of homogenate was used for the estimation of the total ATPase.

Estimation of Mg^{2+} ATPase

The reaction mixture for Mg^{2+} ATPase assay contained 0.5ml of Tris buffer (0.13 M; pH 7.4), 0.4 ml of substrate ATP, 0.5ml of Magnesium chloride (0.05 M) and 0.2 ml of crude homogenate (enzyme source). The contents were incubated at 37°C for 15 minutes and the reaction was stopped by the addition of the 10% TCA. Zero time controls were maintained by adding TCA prior to the addition of homogenate. The contents were centrifuged at 1000g for 15 minutes and the inorganic phosphate was estimated in the supernatant fraction by the method of Fiske and Subba Rao (13).

Estimation of Total ATPase

1% (W/V) homogenate already set apart was used for the total ATPase assay. The reaction mixture in a final volume of 2.6ml contained, 0.5 ml of Tris buffer (0.13 M; pH 7.4), 0.4 ml of substrate ATP, 0.5 ml MgCl_2 (0.05 M), 0.5 ml potassium chloride (0.05 M), 0.5 ml of sodium chloride (0.05M) and 0.2ml of crude homogenate (enzyme source). The contents were incubated at 37°C for 15 minutes and the reaction was arrested by the addition of 1.5 ml of 10% TCA. Zero time controls were maintained by adding TCA prior to the addition of homogenate. The contents were centrifuged and the inorganic phosphate was estimated in the supernatant fraction by the method of Fiske and Subba Rao (13). $\text{Na}^+ \text{K}^+$ ATPase activity was estimated by subtracting the Mg^{2+} ATPase from the Total ATPases. $\text{Na}^+ \text{K}^+$ ATPase = Total ATPases - Mg^{2+} ATPase

Estimation of Inorganic phosphate

The inorganic phosphate in the supernatant fraction was estimated by the method of Fiske and Subba Rao (13). To 1.0 ml of the supernatant, 1.0 ml of ammonium molybdate solution (2.5 gms in 100 ml of 10 N H_2SO_4) was added followed by 0.4 ml of ANSA (1- Amino, 2-Naphol,

4-Sulphonic Acid) (2.5 mgs of ANSA, 97.5 ml of 15% sodium bisulphate and 2.5 ml of 20% sodium sulphate) and allowed to react for 5 minutes. The blue color formed was measured at 660 nm in a UV/VIS spectrophotometer (Hitachi Model) against the reagent blank. The blank contained 2 ml of TCA, 1.0 ml of ammonium molybdate and 0.4 ml of ANSA. The enzyme activity was expressed as μ moles of inorganic phosphate formed/mg protein/hr.

Statistical Treatment of data:

An average of six individual estimations was taken and the mean values of control and experimentals were subjected to statistical analysis. Mean, \pm SD, Percent changes, Two-way ANOVA (14) and 't' tests for multiple comparisons were performed using SPSS Package programming techniques.

Results

Topical exposure of lethal doses of fenvalerate, azadirachtin and synergist to the cockroaches resulted in a gradual, continuous and significant decrease in the activity of the enzyme Na^+K^+ ATPase and Mg^{2+} ATPase (Tab: 1 and 2). The inhibition was dose dependent, time of exposure and tissue specific. Maximum inhibition was observed at 24 hrs of lethal dose exposure in all three chemicals. Na^+K^+ ATP ase activity was decreased more in the nervous tissue compared to muscle (Tab:1), where as maximum inhibition of Mg^{2+} ATP ase was resulted in muscle than to the nervous tissue (Tab:2). Azadirachtin showed less toxic effect than to the synthetic pyrethroid fenvalerate, whereas the synergist is more toxic than the fenvalerate and azadirachtin.

On the other hand sub lethal doses of fenvalerate, azadirachtin and synergist results gradual, continuous and reversible decrease in the activity of Na^+K^+ ATPase and Mg^{2+} ases. In all the tissues maximum decrease was observed at 12hrs of post exposure. There after the enzyme activity showed recovery towards the controls (Tab 3 and 4). The recovery activity was close to the control levels in muscle tissue where as in the nervous tissue the activity remained below the control levels.

Discussion

As ATPases are membrane bound enzymes any damage to cellular organelles due to toxins, heavy metals or pesticides would certainly results in the decreased activity levels. The result of the present study shows that ATPases activity was inhibited tissue specific infirming the differential sensitivity of nervous and muscle tissue to the insecticides. The results also supports that the nervous system is the principle target for the majority of insecticides. Higher levels of Mg^{2+} ATPase observed in muscle than in

the nervous system suggests the greater involvement of enzyme in muscular activity. The decrease in Mg^{2+} ATPase activity might be due to low operation of oxidative metabolism. Similarly Na^+K^+ ATP ase found to be high in the nervous tissue than in the muscle tissue indicates the important role played by this enzyme during nerve conduction. Inhibition of both Mg^{2+} ATPase s and Na^+K^+ ATPases was also reported in Cockroach (15), Rat (16, 17), Rice leaflet larvae (18) and fish (19) with different insecticide such as decamethrin, cypermethrin, fenvalerate, azadirachtin and some synergists. The inhibition of Mg^{2+} ATPases observed in the present study could lead to a reduction in ATP production which in turn would alter Na^+K^+ pump activity, producing neuronal dysfunction. The relative sensitivities of ATPases to all three insecticides indicates that Na^+K^+ ATPase is more sensitive and seems to be a target among the enzyme systems studied (15, 16). The recovery activity in the animals exposed to sub lethal doses of fenvalerate, azadirachtin and the synergist indicates the detoxification mechanism in cockroach to overcome the toxic effects of low doses of these insecticides. The action of pyrethroids can be effectively augmented by various synergists. In this study also the efficacy of fenvalerate was increased when it was combined with azadirachtin.

Conclusion

The synergist though contained 50% of azadirachtin, exerted neurotoxin effects greater and similar to the individual action of fenvalerate. The synergist used in the present study would possibly be an effective insecticide with lesser problems of resistance development, environmental and health hazards.

REFERENCES

1. Dhingra S, Rao GR. J Entomolo Res 2000; 24:115.
2. Israel Stalin S, Kiruba S, Manohar Das. S. Turkish J Fish Aqu Sci 2008; 8:01.
3. Nigel hill. In: Proc Sixth Inter Conf Urban Pests, Eds. Robinson WH, Daniel B. Ook press Hungary, 2008.
4. Takao K. Physiol Rev 1985; 65: 467.
5. Harper AH, Rodwell VW, Mayer P. A. In: Review Physiol Chem. 16th ed. Lange Medical Publications, Maruzen Company Ltd. California, USA. 1977.
6. Lehninger L, Albert. The Molecular Basis of Cell Structure and Function. In: Biochemistry 2nd ed. Kalyani Publishers, New Delhi, 1988.
7. Matsumura, Patil KC. Sci 1969; 166: 121.
8. Singerman, A. Clinical signs Vs biochemical effects for toxic metals. In: Ed. Nordberg, G.F., Effects of Dose and Response, 1976.
9. Tucker RK, Matte A. Bull Environ Contam Toxicol 1980; 24:847.

Table - 1
Alterations in Na⁺ K⁺ ATP are activity (μ moles of Pi formed/mg protein/hr) in the cockroach *Periplanata americana* exposed to lethal doses of fenvalerate, azadirachtin and the synergist

Chemical	Tissue	Post exposure time periods					
		Control	1 Hr	4 Hr	8 Hr	12 Hr	24 Hr
Fenvalerate	Brain PDC	27.84 ± 0.144	24.25 ± 0.136 – 12.89	22.12 ± 0.249 – 20.54	19.54 ± 0.183 – 29.81	17.53 ± 0.094 – 37.03	16.30 ± 0.139 – 41.45
Azadirachtin	Brain PDC	27.84 ± 0.144	25.05 ± 0.394 – 10.04	22.76 ± 0.271 – 18.24	20.34 ± 0.216 – 26.93	19.48 ± 0.216 – 30.03	17.32 ± 0.641 – 37.78
Synergist	Brain PDC	27.84 ± 0.144	23.96 ± 1.163 – 13.94	21.58 ± 0.364 – 23.07	17.22 ± 0.364 – 38.14	12.87 ± 0.133 – 53.77	9.51 ± 0.217 – 65.63
Fenvalerate	VNC PDC	23.02 ± 0.138	20.99 ± 0.149 – 8.81	19.07 ± 0.125 – 17.15	17.08 ± 0.156 – 25.80	14.96 ± 0.088 – 35.01	13.10 ± 0.164 – 43.09
Azadirachtin	VNC PDC	23.02 ± 0.138	22.06 ± 0.166 – 4.17	20.96 ± 0.394 – 12.63	17.81 ± 0.217 – 22.63	16.74 ± 0.714 – 27.28	15.02 ± 0.347 – 34.74
Synergist	VNC PDC	23.02 ± 0.138	20.65 ± 0.133 – 10.29	19.5 ± 0.649 – 14.90	16.78 ± 0.816 – 27.11	14.33 ± 1.063 – 37.74	12.73 ± 0.623 – 44.70
Fenvalerate	Muscle PDC	19.78 ± 0.109	18.62 ± 0.037 – 5.86	18.32 ± 0.32 – 7.38	16.62 ± 0.104 – 15.97	15.61 ± 0.143 – 21.08	14.23 ± 0.132 – 28.05
Azadirachtin	Muscle PDC	19.78 ± 0.109	18.89 ± 0.216 – 4.49	17.94 ± 0.490 – 9.30	17.25 ± 0.221 – 12.79	16.45 ± 0.473 – 16.83	15.52 ± 0.913 – 21.76
Synergist	Muscle PDC	19.78 ± 0.109	18.44 ± 0.263 – 6.77	18.01 ± 0.643 – 8.95	16.48 ± 0.316 – 16.68	15.08 ± 0.139 – 23.76	14.13 ± 1.009 – 28.56

Tab:2 Alterations in Mg⁺ ATP are activity (μ moles of Pi formed/mg protein/hr) in the cockroach *Periplanata americana* exposed to lethal doses of fenvalerate, azadirachtin and the synergist

Chemical	Tissue	Post exposure time periods					
		Control	1 Hr	4 Hr	8 Hr	12 Hr	24 Hr
Fenvalerate	Brain PDC	21.46 ± 0.133	19.42 ± 0.762 – 9.51	16.48 ± 0.136 – 20.21	15.04 ± 0.271 – 29.92	12.77 ± 0.341 – 40.49	11.69 ± 1.061 – 45.52
Azadirachtin	Brain PDC	21.46 ± 0.133	20.72* ± 1.016 – 3.44	18.42 ± 0.863 – 14.21	16.98 ± 0.168 – 20.87	16.34 ± 0.261 – 24.05	15.45 ± 0.663 – 28.00
Synergist	Brain PDC	21.46 ± 0.133	18.78 ± 0.394 – 12.48	17.85 ± 0.163 – 16.82	14.67 ± 0.217 – 32.04	12.25 ± 0.713 – 42.91	10.55 ± 0.096 – 50.83
Fenvalerate	VNC PDC	13.61 ± 0.133	12.10 ± 0.691 – 11.09	10.41 ± 0.261 – 23.51	9.81 ± 0.416 – 27.92	7.69 ± 0.144 – 43.49	6.23 ± 0.261 – 54.22
Azadirachtin	VNC PDC	13.61 ± 0.133	13.11 ± 0.713 – 13.65	11.62 ± 0.216 – 14.62	10.62 ± 0.071 – 21.96	9.72 ± 0.116 – 28.58	9.07 ± 0.116 – 33.35
Synergist	VNC PDC	13.61 ± 0.133	12.50 ± 0.139 – 7.05	11.37 ± 0.264 – 16.45	9.49 ± 0.076 – 30.27	7.19 ± 0.107 – 47.17	5.49 ± 0.216 – 59.66
Fenvalerate	Muscle PDC	24.51 ± 0.161	21.34 ± 0.496 – 12.90	18.43 ± 0.344 – 24.80	15.27 ± 1.491 – 37.69	12.43 ± 0.714 – 49.28	9.41 ± 0.169 – 61.52
Azadirachtin	Muscle PDC	24.51 ± 0.161	22.13 ± 1.096* – 9.71	19.31 ± 0.713 – 21.21	16.46 ± 0.169 – 32.84	14.51 ± 0.133 – 40.77	12.63 ± 0.279 – 48.47
Synergist	Muscle PDC	24.51 ± 0.161	21.02 ± 0.716 – 14.23	17.16 ± 0.139 – 29.98	15.27 ± 1.242 – 37.69	11.98 ± 0.376 – 51.12	8.09 ± 0.216 – 66.98

Each value is a mean ± SD of six individual observations.

PDC = Percent deviation over control, VNC= Ventral Nerve Cord

All the values are significant at P < 0.05-0.001

* Not significant.

Tab:3 Alterations in Na⁺ K⁺ ATP are activity (μ moles of Pi formed/mg protein/hr) in the cockroach *Periplanata americana* exposed to sub lethal doses of fenvalerate, azadirachtin and the synergist

Chemical	Tissue	Post exposure time periods					
		Control	1 Hr	4 Hr	8 Hr	12 Hr	24 Hr
Fenvalerate	Brain PDC	27.84 ± 0.144	25.70 ± 0.144 - 7.68	24.01 ± 0.161 - 13.43	22.50 ± 0.209 - 18.86	21.29 ± 0.164 - 23.53	23.87 ± 0.193 - 14.26
Azadirachtin	Brain PDC	27.84 ± 0.144	26.21 ± 0.207 - 5.85	24.63 ± 0.416 - 11.53	23.34 ± 0.243 - 16.16	22.34 ± 0.713 - 19.75	24.73 ± 1.003 - 11.17
Synergist	Brain PDC	27.84 ± 0.144	25.32 ± 1.163 - 9.06	23.78 ± 1.017 - 14.58	20.59 ± 0.713 - 26.04	17.67 ± 0.168 - 36.53	22.58 ± 0.713 - 18.89
Fenvalerate	VNC PDC	23.02 ± 0.138	21.64 ± 0.153 - 5.99	20.50 ± 0.125 - 10.94	19.77 ± 0.172 - 14.11	17.11 ± 0.139 - 25.67	21.08 ± 0.146 - 8.42
Azadirachtin	VNC PDC	23.02 ± 0.138	22.39* ± 0.364 - 2.74	21.41 ± 0.373 - 6.98	19.40 ± 0.133 - 15.72	18.90 ± 0.261 - 17.89	21.86 ± 0.096 - 5.03
Synergist	VNC PDC	23.02 ± 0.138	21.56 ± 0.133 - 6.46	20.20 ± 0.649 - 12.25	18.70 ± 0.649 - 18.77	14.33 ± 1.063 - 26.62	12.73 ± 0.623 - 9.16
Fenvalerate	Muscle PDC	19.78 ± 0.109	18.97 ± 0.099 - 4.09	18.72 ± 9.166 - 5.32	18.22 ± 0.104 - 7.89	17.49 ± 0.117 - 11.58	18.14 ± 0.20 - 8.29
Azadirachtin	Muscle PDC	19.78 ± 0.109	19.04* ± 0.133 - 3.74	18.94 ± 0.316 - 4.24	18.48 ± 0.094 - 6.58	17.70 ± 0.126 - 10.51	18.62 ± 0.714 - 5.85
Synergist	Muscle PDC	19.78 ± 0.109	18.86 ± 0.165 - 4.65	18.24 ± 0.431 - 7.78	18.01 ± 0.763 - 8.95	17.07 ± 0.634 - 13.70	18.11 ± 1.363 - 8.45

Tab:4 Alterations in Mg⁺ ATP are activity (μ moles of Pi formed/mg protein/hr) in the cockroach *Periplanata americana* exposed to sub lethal doses of fenvalerate, azadirachtin and the synergist

Chemical	Tissue	Post exposure time periods					
		Control	1 Hr	4 Hr	8 Hr	12 Hr	24 Hr
Fenvalerate	Brain PDC	21.46 ± 0.133	20.58 ± 0.141 - 4.56	18.94 ± 0.167 - 11.75	17.72 ± 0.184 - 17.44	16.89 ± 0.169 - 21.29	19.10 ± 0.204 - 10.98
Azadirachtin	Brain PDC	21.46 ± 0.133	20.97* ± 0.517 - 2.28	19.49 ± 0.413 - 9.17	18.01 ± 0.319 - 16.07	17.41 ± 0.913 - 18.87	19.71 ± 0.136 - 8.16
Synergist	Brain PDC	21.46 ± 0.133	19.19 ± 0.264 - 10.57	18.55 ± 0.198 - 13.56	16.38 ± 0.277 - 23.67	16.17 ± 0.317 - 24.65	18.97 ± 0.216 - 11.60
Fenvalerate	VNC PDC	13.61 ± 0.096	12.85 ± 0.142 - 5.54	12.00 ± 0.139 - 11.82	11.49 ± 0.161 - 15.54	10.94 ± 0.161 - 19.61	12.73 ± 0.409 - 6.51
Azadirachtin	VNC PDC	13.61 ± 0.097	13.16* ± 0.294 - 3.29	12.35 ± 0.160 - 9.29	11.76 ± 0.713 - 13.60	11.19 ± 0.516 - 17.78	12.93 ± 0.133 - 4.99
Synergist	VNC PDC	13.61 ± 0.096	12.59 ± 0.107 - 7.51	11.89 ± 0.217 - 12.63	10.32 ± 0.169 - 24.17	10.12 ± 0.334 - 25.64	12.43 ± 0.139 - 8.67
Fenvalerate	Muscle PDC	24.51 ± 0.161	22.67 ± 0.104 - 4.11	20.40 ± 0.063 - 16.76	18.72 ± 0.139 - 23.62	17.14 ± 0.119 - 30.05	21.04 ± 0.091 - 15.98
Azadirachtin	Muscle PDC	24.51 ± 0.161	22.80 ± 9.317 - 6.97	21.16 ± 0.493 - 13.66	19.76 ± 0.713 - 19.35	17.92 ± 0.139 - 26.88	21.94 ± 0.136 - 10.44
Synergist	Muscle PDC	24.51 ± 0.161	21.51 ± 1.073 - 12.23	20.21 ± 0.973 - 17.54	17.49 ± 0.163 - 28.64	16.20 ± 0.271 - 33.904	20.16 ± 1.016 - 17.74

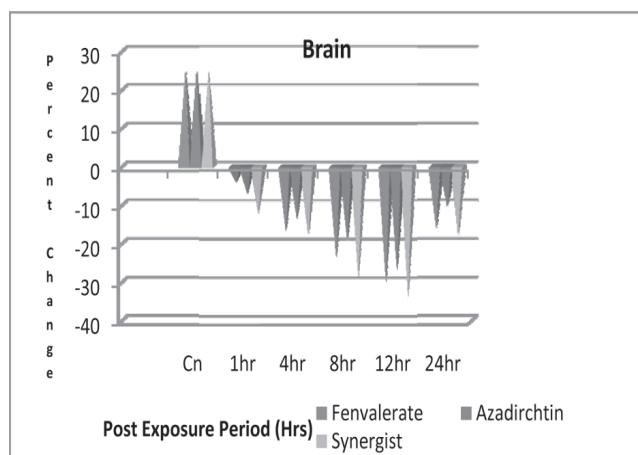
Each value is a mean ± SD of six individual observations.

PDC = Percent deviation over control, VNC= Ventral Nerve Cord

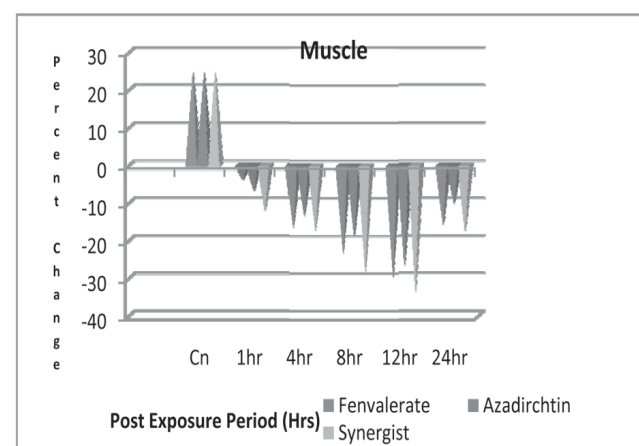
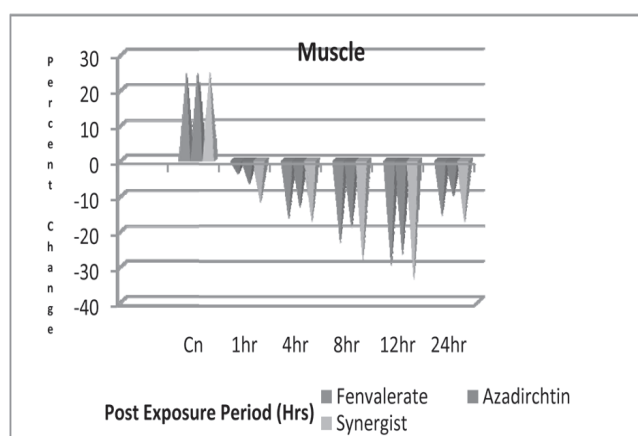
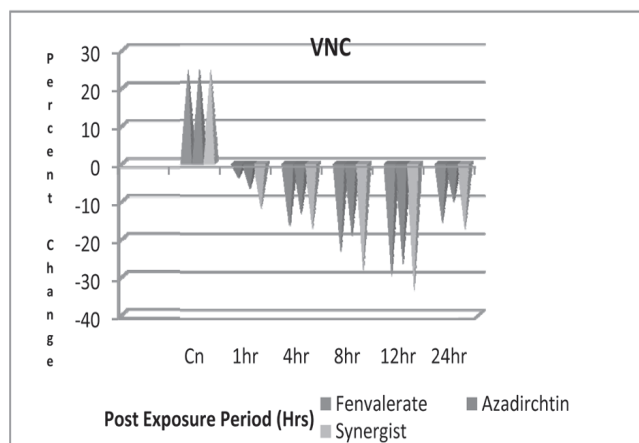
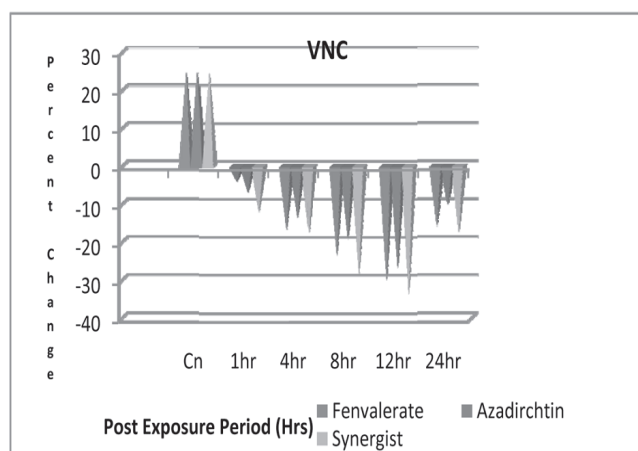
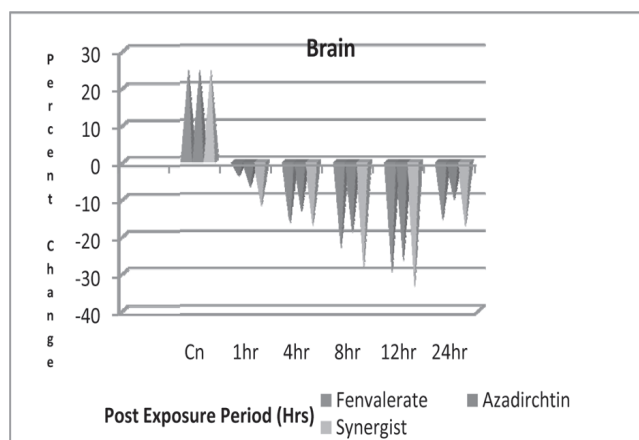
All the values are significant at P < 0.05-0.001

* Not significant.

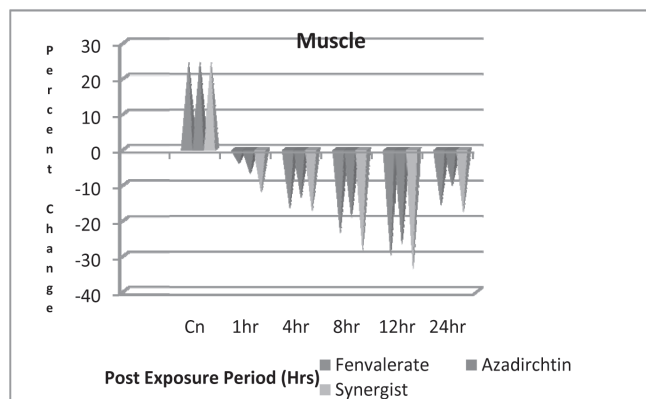
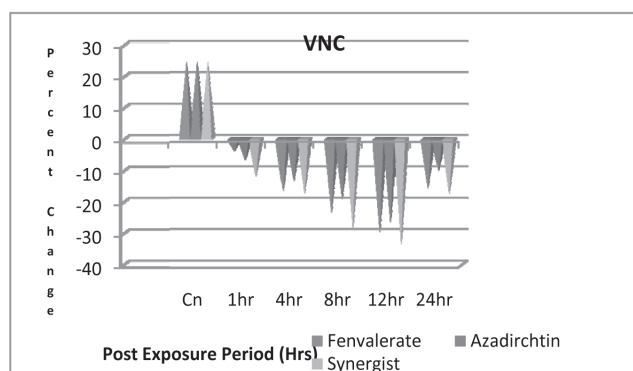
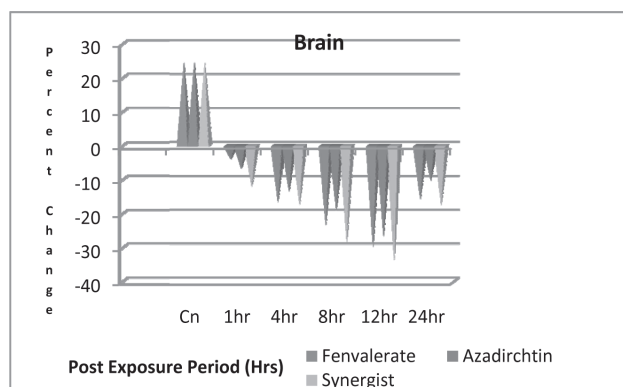
Tab 1: Alterations in $\text{Na}^+ \text{K}^+ \text{ATP}$ are activity (μ moles of Pi formed/mg protein/hr) in the cockroach *Periplanata americana* exposed to lethal doses of fenvalerate, azadirachtin and the synergist



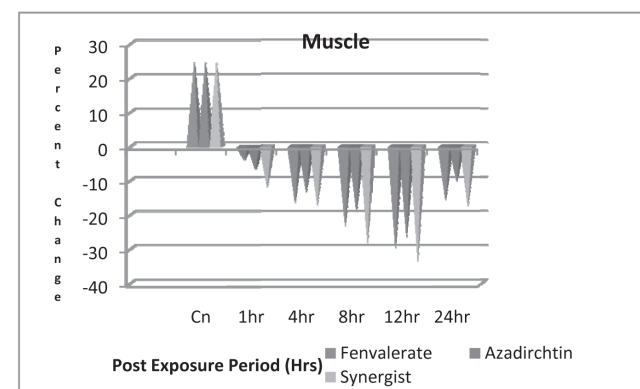
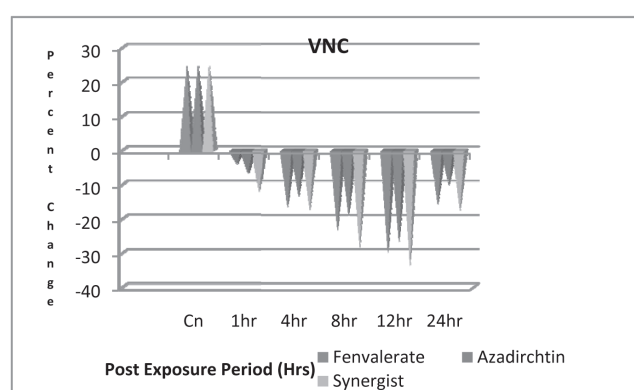
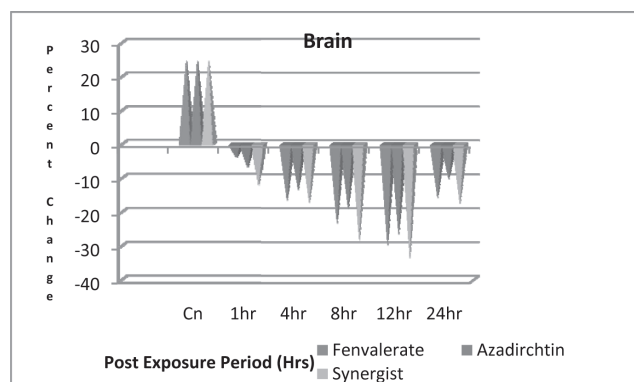
Tab:2 Alterations in $\text{Mg}^+ \text{ATP}$ are activity (μ moles of Pi formed/mg protein/hr) in the cockroach *Periplanata americana* exposed to lethal doses of fenvalerate, azadirachtin and the synergist



Tab:3 Alterations in Na⁺ K⁺ ATP are activity (μ moles of Pi formed/mg protein/hr) in the cockroach *Periplanata americana* exposed to sub lethal doses of fenvalerate, azadirachtin and the synergist



Tab:4 Alterations in Mg²⁺ ATP are activity (μ moles of Pi formed/mg protein/hr) in the cockroach *Periplanata americana* exposed to sub lethal doses of fenvalerate, azadirachtin and the synergist



10. Carfagna MA, Ponsler GD, Muhoberac BB. Chem. Biol. Interact 1996; 100:53.
11. Reddy GR, Shafeek A, Chetty CS, Sajwan KS. 9th International Congress of Toxicology, Brisbane, Australia 2001.
12. Tirri R, Lagarspetz KYH, Kohonen, J Comp Biochem Physiol 1973; 44:473.
13. Fiske CH, Subbaro Y. J Biol Chem 1925; 66:375.
14. Steel, R. D. G and J. M. Torrie. Principles and procedures of statistics with special reference to the biological sciences.

- McGraw Hill Book Inc., New York. 1960: 481.
15. Reddy GR, Madhusudhana L, Shafeek A, Chetty CS Bull Eviorn Contam Toxicol 2001; 45:416.
16. Grosman N, Diel F. Int Immune Pharmacol 2005; 5:263.
17. Siraj Mohiyuddin S, Rajeswar Reddy S, Anand Kumar L, Jacob Doss P. The Bioscan 2010; 5:153.
18. Senthil Nathan S, Kalaivani K, Murugan K, Chung PG. Pesticide Biochem Physiology 2005; 81:113.
19. Kumar S. Inter J Bio Eco Environ Sci 2009; 1:1.



Design and Development of Transdermal Patches for Verapamil Hydrochloride

P. SRIKANTH REDDY¹, D. SARITHA², M. RAVI KUMAR³ AND K.N. JAYAVEERA⁴

¹Department of Pharmaceutics, MNR College of Pharmacy, Sangareddy, India.

²Department of Pharmaceutics, Sultan-ul-uloom College of Pharmacy, Hyderabad, India.

³Department of Pharmaceutics, Geethanjali College of Pharmacy, Keesara, Hyderabad.

⁴Chairman & CEO, Science-tech foundation, Bengaluru.

ABSTRACT

Verapamil hydrochloride is an antihypertensive agent which undergoes extensive first pass metabolism making it a possible candidate for transdermal delivery. Patches were prepared using hydroxypropylmethylcellulose, eudragit RL 100, sodium carboxymethyl cellulose and carbopol. The results of FTIR and DSC revealed no interaction between drug and polymers. The loss of moisture and uptake of moisture were within the limits. The formulations showed an extended release of the drug upto period of 24 hours during *in vitro* permeation studies and showed non Fickian drug release. Stability of the optimized formulation was investigated as per ICH guidelines and was found to be stable with respect to drug content and *in vitro* permeation.

Key words: *In vitro* permeation, Franz diffusion cell, moisture uptake, non Fickian diffusion, Verapamil.

Introduction

Transdermal administration refers to continuous drug infusion through an intact skin surface to control the delivery of drug [1]. Transdermal drug delivery is a non-invasive delivery of medicament from the surface of the skin [2]. This has advantages over the oral route of administration, in patient compliance and bypassing first pass metabolism. Several drugs were explored for the possible use in transdermal drug delivery for treating hypertension. A few of these are: nifedipine [3], metoprolol [4] and isradipine [5].

Verapamil is an effective calcium channel blocker, used in the treatment of angina, hypertension and myocardial infarction. It was reported to be rapidly absorbed after oral administration, but undergoes extensive first pass metabolism leading to poor bioavailability (20%). In addition, verapamil has low dose (30 mg), low molecular weight, 491, and lipophilic in nature (log P, 3.28); needed for long term treatment and repetitive dosing. All these parameters make this drug an interesting candidate for transdermal drug delivery [6-9].

Materials and Methods

Verapamil hydrochloride was a gift from Nicholas Piramil Healthcare Ltd., (Kohir, India). Eudragit was generous gift from Colorcon Asia PVT Ltd., (Goa, India); Carbopol, HPMC, SCMC were gifted by Inventis drug delivery systems PVT Ltd., (Hyderabad, India). All reagents were used of analytical grade.

Animals

Male Wistar rats weighing approximately 200 – 250 g were used for the diffusion studies of verapamil transdermal patches. The animals were supplied with food and water ad libitum. The animal studies were approved by the Institute Animal Ethics Committee (IAEC), Regd no. 1434/PC/a/11/ CPCSEA and all experiments were conducted as per the norms of the Committee for the Purpose of Supervision of Experiments on Animals, India.

Investigation of drug–excipient interactions

Fourier transform infrared spectroscopy

Compatibility between drug and the polymers were studied by FTIR spectra. FTIR studies were carried out for drug and its physical mixture (1:1). The sample was dispersed in KBr powder and the pellets were made by applying 6000 kg/cm² pressure and analyzed. FTIR spectra were obtained by diffuse reflectance on a FTIR

*Address for correspondence:
poreddysrikanthreddy@gmail.com

spectrophotometer type FTIR 8400 (Schimadzu Corporation, Japan). The positions of FTIR bands of important functional groups of drug were identified and were cross checked in obtained spectra [10].

Differential scanning calorimetry (DSC)

DSC studies for drug and its physical mixture (1:1) were carried out using DSC-60 calorimeter (Schimadzu Corporation, Japan). The instrument was calibrated with an indium and zinc standard. The sample was heated from 10 to 300°C at a heating rate of 25°C/min to remove thermal history. The sample was then immediately cooled to 10°C and reheated from 10 to 300°C under the flow of nitrogen at a heating rate of 10°C/min.

Preparation of patches

Verapamil transdermal films were prepared by solvent casting technique using Carbopol, SCMC, HPMCK15M, eudragit and carbopol as polymers. Glycerine and polysorbate 80 were used as plasticizer and penetration enhancer respectively. Ethanol, methanol and DCM were used as solvents. Drug was dissolved in little quantity of solvent and polymers were dissolved in remaining solvent/solvent mixture. Drug, polymer solutions along with plasticizer and permeation enhancer were sonicated for 30 min and examined for air entrapment. The solution was poured onto glass moulds of 10 × 5 cm² and air dried for overnight at room temperature. An inverted funnel was kept on the mould for controlled evaporation. The dried film of the drug was peeled from the mould and packed in aluminium foil and kept in desiccator till further use.

Thickness

Thickness of patches was measured using a micrometer (Mitutoyo co., Japan) for a pack of 5 films. Mean ± standard deviation was calculated [11].

Weight Variation

Ten patches (1×1 cm²) were selected and weight variation was evaluated for each formulation [12].

Folding Endurance

Each patch was folded repeatedly several times at the same place until the patch breaks. The first appearance of breaking was observed and then the folding endurance was reported by the number of foldings before it was broken [13].

Loss of Moisture

The patches were initially weighed (W1) individually and placed in a dessicator (containing activated silica) at room temperature (30 ± 0.5 °C). After three days, the films were taken out and weighed (W2). Percent loss of moisture was calculated using formula, given below [14].

$$\% \text{ Loss of Moisture} = W1 - W2 / W2 \times 100$$

Moisture Uptake

The patches were weighed (W1) and placed in a dessicator (containing 100 ml saturated solution of sodium chloride, 75% RH) at room temperature (30 ± 0.5 °C). After three days, the films were removed and weighed (W2). Percent gain of moisture was calculated using the given formula [15],

$$\% \text{ Gain of moisture} = W1 - W2 / W2 \times 100$$

Drug Content

Drug content of patches was determined by dissolving five patches (1 cm²) in 100 ml of 7.4 buffer. After suitable dilutions the resultant solution was filtered and analysed for verapamil content spectrophotometrically [6-9].

Table 1
Composition of verapamil patches

Ingredients	Formulation code			
	F 1	F 2	F 3	F 4
Verapamil (mg)	500	500	500	500
HPMC K15M (mg)	900	600	600	600
SCMC (mg)	—	300	—	—
Eudragit RL 100 (mg)	—	—	300	—
Carbopol 934P (mg)	—	—	—	300
Dimethylsulphoxide (ml)	0.2	0.2	0.2	0.2
Propylene glycol (ml)	0.4	0.4	0.4	0.4
Ethanol (ml)	—	5	—	5
Methanol (ml)	7.5	5	7.5	5
Dichloromethane (ml)	7.5	5	7.5	5

HPLC analysis

Analysis of samples was performed using a Shimadzu 10 AVP (Japan) HPLC system equipped with UV detector and waters C-18 column (300 × 4.6 mm i.d) at ambient temperature. The mobile phase was mixture of 700 ml of phthalate buffer pH 2.8 and 250 ml of acetonitrile. The solution was filtered through 0.45 µm filter and degassed by sonication. The flow rate was 1 ml per minute. Detection was carried on at 275 nm wavelength. A calibration curve was plotted for verapamil in the range of 10-50 µg/ml. A good linear relationship was observed between the concentration of verapamil and its peak area ($r^2 = 0.9972$). Precision and accuracy of the HPLC method were estimated [16].

In vitro Permeation Studies using Rat Skin:

Franz diffusion cell was used for *in vitro* skin permeation studies. The skin of the rat abdominal region was used. The preparation of skin for diffusion study was as follows. Male wistar rats weighing 200-250 g were used. The rats were anaesthetised using chloroform and the abdomen was carefully shaved with scissors and razor [17]. Full thickness skin (i.e., epidermis, subcutaneous and dermis) was excised from the abdominal site [18]. Any skin with damages was rejected. The skin sample was placed in the Franz diffusion cell. Slightly larger skin was taken to help its fixation on the diffusion cell. The patch of area 3.14 cm² was used. The receptor compartment was filled with phosphate buffer, pH 7.4. Samples of one ml were withdrawn at predetermined time intervals and one ml was replaced with fresh solution. Required dilutions were made for the sample and the amount of drug that reached receptor compartment was analyzed for drug content using HPLC and the data was statistically analysed by one way ANOVA followed by turkey post hoc test for multiple comparison using graph pad prism. Differences were considered to be significant at a level of $p < 0.05$.

The permeability coefficients (P) were calculated as follows [19]

$$P = (dQ/dt) / (CA)$$

Where

- dQ/dt - Permeation rate,
- C - Concentration of the donor chamber
- A - Surface area of diffusion

Steady state fluxes (J_{ss}) were calculated by dividing the slope of cumulative amount permeated Vs time curve by the diffusional area.

Stability studies

Stability studies were conducted according to the ICH Q1A (R2) guidelines. Patches were wrapped in aluminum foil and were kept in stability chamber at a temperature of 40±2°C and 75±5% RH for 6 months [20]. Samples were withdrawn at the end of 6 months and analyzed for drug

content and *in vitro* permeation. Zero time samples were used as control for the study and the results were statistically analyzed by using t-test and $p < 0.05$ were considered as significant.

Results & Discussion

Investigation of drug-excipient interactions

FTIR spectral analysis

Verapamil pure drug and its formulations were subjected to FTIR spectroscopic analysis. The obtained spectra are shown in figure 1. The FTIR spectra of pure Verapamil showed sharp characteristic peaks at 1261 (C–O stretch), 1591, 1518 (Bands due to skeletal vibrations of the benzene ring), 2235 (C=N stretch), 2578, 2542, 2453 (N–H stretch) and 2839, 2956, 2937 cm⁻¹ (C–H stretch). All the above characteristic peaks appeared in the spectra of formulations at the same wavenumbers indicating no modification or interaction between the drug and polymers.

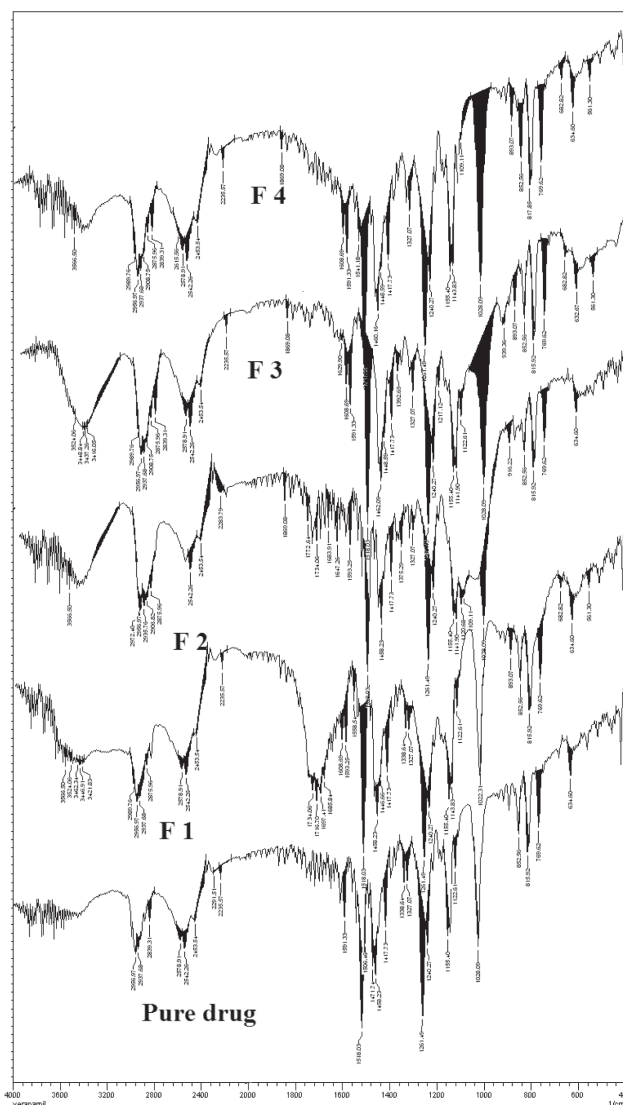


Fig.1: FTIR spectra of verapamil and its formulations

Differential scanning calorimetry

DSC studies were carried out for verapamil pure drug, physical mixture and its formulations. DSC thermograms of verapamil and its formulations are shown in figure 2. The melting point of verapamil is 140-144°C. The DSC thermogram of verapamil showed an endothermic peak at 144.32°C corresponding to its melting temperature, which was also detected in the thermograms of formulation, signifying no change in crystal form and interaction between the polymers.

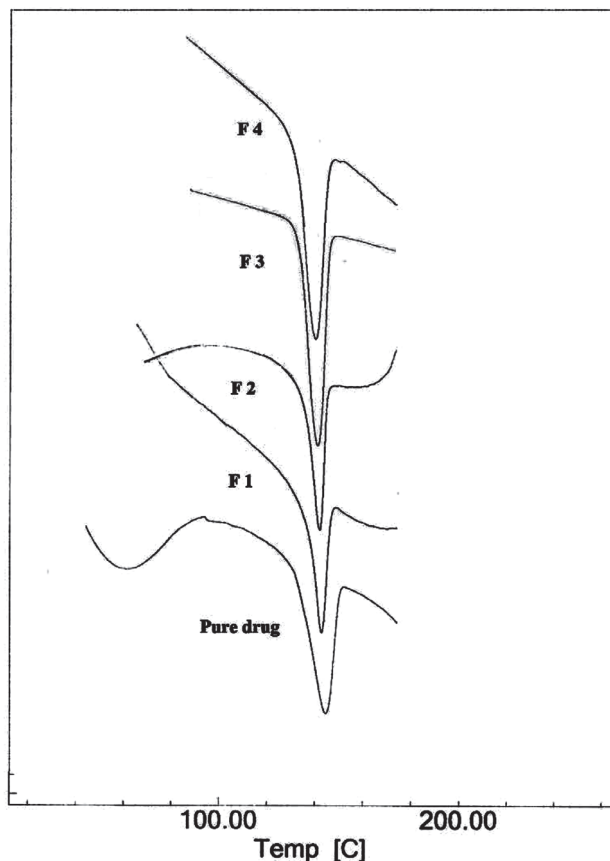


Fig.2 : DSC thermograms of verapamil and its formulations

Physicochemical evaluation of verapamil patch

The % drug content of patches was found to be 98.27 ± 1.37 , 98.5 ± 1.51 , 98.63 ± 0.76 and 98.33 ± 1.56 for the

formulations F 1, F 2, F 3 and F 4 respectively. The weight of the patches was found to be 26.22 ± 0.35 mg, 27.09 ± 0.18 mg, 28.28 ± 0.47 mg and 27.28 ± 0.16 mg for the formulations F 1, F 2, F 3 and F 4 respectively. The thickness was found to be 281 ± 2.08 μ m, 246 ± 1.52 μ m, 249 ± 2.00 μ m and 261 ± 2.51 μ m for the formulations F 1, F 2, F 3 and F 4 respectively. The mean folding endurance values were found to be 181 ± 9.16 , 213 ± 7.02 , 273 ± 2.51 and 223 ± 7.5 for the formulations F 1, F 2, F 3 and F 4 respectively. Folding endurance of the patches was in the order F 3>F 2>F 4>F 1. F 3 showed maximum folding endurance may be due to the presence of eudragit. The folding endurance of all the patches was optimum, the patches exhibited good physical and mechanical properties. The overall moisture uptake was low ($\sim 10\%$), which was satisfactory for the patches. Thus the general physical properties are satisfactory.

In vitro permeation studies

In vitro permeation studies for the patches were carried out in triplicate and after 24 hours the release was found to be 76.19 ± 6.01 , 92.71 ± 7.81 , 66.46 ± 5.71 and $83.63 \pm 5.81\%$ for the formulations F 1, F 2, F 3 and F 4 respectively (figure 3). The data of *In vitro* permeation was analyzed by one way ANOVA and significant difference was observed between the means. *In vitro* permeation study of formulation F 2 showed a maximum release of the drug, $92.71 \pm 7.81\%$ in 24 hr and this formulation was considered as optimized one and used for further study. The order of drug release is F 2>F 4>F 1>F 3.

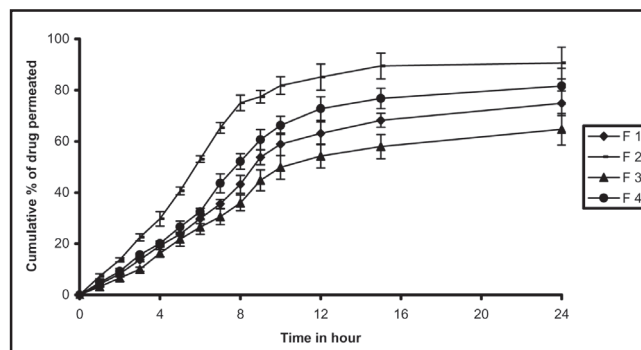


Fig. 3 : *In vitro* permeation profile of verapamil patches

Formulation containing SMC (F 2) showed maximum swelling and a gel layer was formed on the surface which

Table 2

Physical evaluation of verapamil patches

Formulation	Parameter					
	% Drug content	Weight variation (mg)	Thickness (μ m)	Folding endurance	Moisture Uptake(%)	Loss of moisture(%)
F 1	98.27 ± 1.37	26.22 ± 0.35	281 ± 2.08	181 ± 9.16	2.06 ± 0.53	2.34 ± 1.16
F 2	98.5 ± 1.51	27.09 ± 0.18	246 ± 1.52	213 ± 7.02	4.78 ± 0.13	3.13 ± 1.32
F 3	98.63 ± 0.76	28.28 ± 0.47	249 ± 2.00	273 ± 2.51	3.5 ± 0.71	2.97 ± 0.91
F 4	98.33 ± 1.56	27.28 ± 0.16	261 ± 2.51	223 ± 7.50	1.75 ± 0.06	1.2 ± 0.16

may be due to more hydrophilic nature of SCMC. When swelling is prevalent, drug diffusion may occur through the solvent-filled pathways of swollen patch. Erosion of polymer matrix can also affect the drug release. The loosely bound polymer molecules in these patches eroded readily, allowing faster release of verapamil from the patches. F 4, shows slow release of the drug which may be due to the high viscous nature of HPMC K15M. In addition, HPMC K15M forms a thick gel (diffusion path length) that acts as a barrier for drug diffusion and prevents matrix disintegration and additional water penetration. Formulation F 4 showed faster release, which may be due to presence of carbopol and HPMC. Carbopol undergo ionization and activates negative charges at the backbone of polymer. Repulsion between these like charges leads to uncoiling of the polymer to produce an extended structure capable of greater uptake of water. Thus owing to generation of pores by HPMC and uncoiling of carbopol, the system absorbs more water and there by promotes diffusion, which in turn leads to an increase in release of drug. Presence of eudragit in formulation F 3 slower the drug release, which may be due to water insolubility of eudragit, lower dissolution and slower erosion of films.

The drug release data obtained were fitted in to zero order, first order, Higuchi and Korsmeyer-Peppas equations to know the mechanism of drug release from these formulations. The *in vitro* permeation profile of F 1 & F 2 formulations could be best expressed by Korsmeyer-Peppas model, as the plots showed highest linearity (r^2 : 0.9941 & 0.9904 respectively) and F 3 & F 4 formulation could be best expressed by zero order model, as the plots showed highest linearity (r^2 : 0.997 & 0.9927 respectively). All the

formulations showed a non- Fickian release pattern as it was evidenced from the release exponent ($n > 0.5$) (table 3). This indicates coupling of the diffusion and erosion mechanism, called anomalous diffusion and shows that the drug release is controlled by more than one process. So, the suggested drug release mechanism for verapamil patches may be combination of diffusion and erosion of polymer matrix.

The mean steady state flux (J_{ss}) was found to be 0.6229 ± 0.04 , 0.771 ± 0.05 , 0.5358 ± 0.02 , 0.7003 ± 0.05 mg/cm²/hr and the permeability coefficient was found to be 0.0771 ± 0.01 , 0.0536 ± 0.002 , 0.07 ± 0.01 , 0.0623 ± 0.004 cm/hr for the formulations F 1, F 2, F 3 and F 4 respectively.

Stability studies

Accelerated stability studies were performed for optimized formulation (F 2) as per ICH Q1A (R2) guidelines at $40 \pm 2^\circ\text{C}$ and $75 \pm 5\%$ RH for 6 months. After specified duration, visual examination of the patches did not show any change in morphology. The results of the stability studies revealed that there were no significant changes in drug content and *in vitro* permeation. The cumulative percentage of verapamil permeated in 12 h was found to be $84.93 \pm 3.56\%$. Flux and permeability coefficient of verapamil was found to be 0.7235 ± 0.05 mg/cm²/hr and 0.072 ± 0.01 cm/hr respectively for the optimized formulation after stability study.

Conclusion

Transdermal patches of verapamil were prepared by solvent evaporation technique. The patches exhibited good physical properties. The *in vitro* permeation patches was

Table-3

Correlation coefficient (r^2) and rate constant of different kinetic models for verapamil patches

Formulation	n value	Correlation coefficient (r^2)				Drug transport mechanism
		Zero order	First order	Higuchi	Peppas	
F 1	0.9098	0.9937	0.9651	0.9555	0.9941	Non - Fickian diffusion
F 2	0.8317	0.9529	0.9869	0.9790	0.9904	Non - Fickian diffusion
F 3	0.9440	0.9970	0.9768	0.9593	0.9956	Non - Fickian diffusion
F 4	0.8641	0.9927	0.9663	0.9601	0.9917	Non - Fickian diffusion

Table - 4

***In vitro* permeation flux and permeability coefficient of verapamil patches**

Formulation	Flux (J_{ss}) (mg/cm ² /hr)	Permeability coefficient (cm/hr)
F 1	0.6229 ± 0.04	0.0623 ± 0.004
F 2	0.771 ± 0.05	0.0771 ± 0.01
F 3	0.5358 ± 0.02	0.0536 ± 0.002
F 4	0.7003 ± 0.05	0.07 ± 0.01

attempted using Franz diffusion cell, with and rat skin. Good results were obtained both *in vitro* conditions for patches. The statistical investigation of *in vitro* permeation data showed that the coupling of the diffusion and erosion is the mechanism of drug release. From the present investigation, it can be concluded that transdermal patches of verapamil may provide sustained delivery for prolonged periods in the management of hypertension, which can be a good way to bypass the extensive hepatic first-pass metabolism.

Acknowledgement

The authors are thankful to M/s Nicholas Piramil Healthcare Ltd., Kohir, India for providing gift sample of verapamil hydrochloride. The authors are thankful for MNR educational trust, Hyderabad for providing support in carrying out the research work.

References

- Chien YW, Transdermal therapeutic systems, In: Robinson JR, Vincent HL, editors. Controlled drug delivery fundamentals and applications. 2nd ed., New York: Marcel Dekker, Inc. 1987: 523.
- Misra AN, Transdermal drug delivery. In: Jain NK, editors. Controlled and novel drug delivery. New Delhi: India: CBS Publisher and distributor. 1997: 100.
- Sankar V, Johnson DB, Sivanan V, Ravichandran V, Raghuraman SR, Design and evaluation of nifedipine transdermal patches, Indian J Pharm Sci. 2003; 65: 510.
- Sadhana PG, Jain SK, Effective and controlled transdermal delivery of metoprolol tartrate, Indian J Pharm Sci. 2005; 67: 346.
- Saleh A, Al-swayeh, Effect of penetration enhancers on the transdermal delivery of isradipine through excised rabbit skin, Saudi Pharmaceutical Journal. 2008; 16:155.
- Indian Pharmacopoeia, Ministry of Health and Family welfare, The Indian Pharmacopoeia commission, Ghaziabad, 6th edition 2010: 2295.
- <http://www.rxlist.com/cardizem-la-drug/clinical-pharmacology.htm>.
- Nehal A. Kasim, Marc Whitehouse, Chandrasekharan Ramachandran, Marival Bermejo, Hans Lennernas, Ajaz S. Hussain, Hans E. Junginger, Salomon A. Stavchansky, Kamal K. Midha, Vinod P. Shah and Gordon L. Amidon, Molecular properties of WHO essential drugs and provisional biopharmaceutical classification, Mol Pharm. 2003;1: 85.
- Maria Irene Yoshida, Elionai Cassiana Lima Gomes, Cristina Duarte Vianna Soares, Alexandre Frinhani Cunha and Marcelo Antonio Oliveira, Thermal analysis applied to verapamil hydrochloride characterization in pharmaceutical formulations, Molecules. 2010; 15: 2439.
- Klaus Florey, Analytical profiles of drug substances and excipients, Academic press, Sandiego, USA, 2000: 643.
- Amnuakitt C, Ikeuchi .I, Ogawara K, Higaki K and Kimura T, skin permeation of propranolol from polymeric film containing terpene enhancers for transdermal use, Int J Pharm. 2005; 289:167.
- Verma PRP and Iyer SS, Transdermal delivery of propranolol using mixed grades of Eudragit: design and in vitro and in vivo evaluation, Drug Dev Ind Pharm. 2000; 26: 471.
- Devi VK, SaishivamS, Maria GR, Deepti PU. Design and evaluation of matrix diffusion controlled transdermal patches of verapamil hydrochloride, Drug Dev Ind Pharm. 2003; 29: 495.
- Jamkhani VG, Mulla JS, Vinay BL, Shivakumar HN, Formulation, characterization and evaluation of matrix – type transdermal patches of a model antihypertensive drug, Asian Journal of Pharmaceutics. 2009; 1: 59.
- Saxena M, Mutalik S, Reddy MS, Formulation and evaluation of transdermal patches of metaclopramide hydrochloride, Indian Drugs. 2006; 43: 740.
- Bright A, Renuga Devi TS, Gunasekaran S. Application of RP-HPLC and UV-Visible Spectroscopy for the Estimation of Atenolol and Verapamil in Tablets Before and After the Expiry Period, Int J Chem Tech Res. 2010; 2: 860.
- Gupta JRD, Irchhiaya R, Garud N, Priyanka T, Prashanth D, Patel JR, Formulation and evaluation of matrix type transdermal patches of glibenclamide, International Journal of Pharmaceutical Sciences and Drug Research. 2009; 1: 46.
- Ligang Zhao, Liang Fang, Yongnan Xu, Transdermal delivery of penetrants with differing lipophilicities using O – acylmenthol derivatives as penetration enhancers, European Journal of Pharmaceutics and Biopharmaceutics. 2008; 69: 199.
- Shojaei AH, Zhou SL, Li X. Transbuccal Delivery of Acyclovir (II): Feasibility, System Design, and *In Vitro* Permeation Studies, J Pharm Pharmaceut Sci. 1998; 1: 66.
- Saranjit Singh. Drug stability testing and shelf-life determination according to international guidelines, Pharmaceutical technology. 1999; 23: 68.



INSTRUCTION TO AUTHORS

GENERAL REQUIREMENTS: Journal of Pharmacy and Chemistry (ISSN 0973-9874) is a quarterly Journal, *Indexing in CAS(Coden:JPCOCM)* which publishes original research work that contributes significantly to further the scientific knowledge in Pharmaceutical Sciences (Pharmaceutical Technology, Pharmaceutics, Biopharmaceutics, Pharmacokinetics, Pharmaceutical Chemistry, Computational Chemistry and Molecular Drug Design, Pharmacognosy and Phytochemistry, Pharmacology, Pharmaceutical Analysis, Pharmacy Practice, Clinical and Hospital Pharmacy, Cell Biology, Genomics and Proteomics, Pharmacogenomics, Stem Cell Research, Vaccines & Cera, Bioinformatics and Biotechnology of Pharmaceutical Interest) and in Chemical Sciences (Inorganic, Soil, Forensic, Analytical, Nano, Environmental, Polymer, Physical, Agricultural, Medicinal, Biochemistry, Organic, Computational, Food, Pesticides etc). Manuscripts are accepted for consideration by Journal of Pharmacy and Chemistry on the condition that they represent original material, have not been published previously, are not being considered for publication elsewhere, and have been approved by each author. Review articles, research papers, short communication and letters to the editor may be submitted for publication.

SUBMISSION OF MANUSCRIPTS: Typewritten manuscripts prepared using MS Word should be submitted in triplicate and RW-CD to Prof. Dr. K.N Jayaveera, Editor-in-Chief of Journal of Pharmacy and Chemistry, Plot No 22, Vidyut Nagar, Ananthapur- 515 001, Andhra Pradesh, India. e-mail: editorjpc@gmail.com

All components of the manuscript must appear within a single electronic file: references, figure legends and tables must appear in the body of the manuscript.

TYPING INSTRUCTION: The following detailed instructions are necessary to allow direct reproduction of the manuscript for rapid publishing. If instructions are not followed, the manuscript will be returned for retyping. The following typefaces, in 12 points size, are preferred: Times Roman.

GENERAL FORMAT: The typing area must be exactly 6 5/8" (168 mm) wide by 9 7/8" (250 mm) long. Justify margins left and right (block format). The entire typing area of each page must be filled, leaving no wasted space. Text should be double-spaced, special care should be taken to insure that symbols, superscripts and subscripts are legible and do not overlap onto lines above or below. Make sure text lines are equidistant.

TITLE: On the first page of the manuscript, start title 1" (25 mm) down from top text margin. Type title in all capital letters, centred on the width of the typing area and single-spaced if more than one line is required. The title should be brief, descriptive and have all words spelled out. Double-space, then type the author(s) name(s), single-spaced if more than one line is required. Double-space, than type author(s)

address(es), single-spaced, capitalizing first letters of main words. Quadruple-space before Abstract.

ABSTRACT: Centre, type and underline abstract heading, capitalizing the first letter. A double-space should separate the heading from the abstract text. Indent abstract text approximately 1/2" (13 mm) from both left and right margins. The abstract should be intelligible to the reader without reference to the body of the paper and be suitable for reproduction by abstracting services. Introduction to the text (without a heading) should be four spaces below the abstract using full margins.

KEY WORDS: Three or more key words must be provided by authors for indexing of their article. Key words will be listed directly below the Abstract. Abbreviated forms of chemical compounds are not acceptable. Spell out entirely, using the official nomenclature. Example: L-dihydroxyphenylalanine (L-DOPA)

MAJOR HEADINGS: Papers must include the major headings: Introduction, Methods, Results, Discussion, Acknowledgments and References. Capitalize first letter, underline, and centre headings on width of typing area.

TABLES/FIGURES: Incorporate tables and/or figures (B & W) with their legends into the main body of text.

REFERENCES: References should be referred to a number [1] in the text and be listed according to this numbering at the end of the paper. Only papers and books that have been published or in press may be cited; unpublished manuscripts or manuscripts submitted to a journal but which have not been accepted may not be cited.

The references should comprise the following information and in the given order and with given punctuation as given in the example below: Author name (s), Initials (s), Publication Title, Page Number, Year of Publication.

Standard Journal Article:

- [1] Bhattacharyya D, Pandit S, Mukherjee R, Das N, Sur TK. Indian J Physiol Pharmacol 2003; 47:435.
- [2] Skottova N, Krecman V. Physiol Res 1998; 47:1.

Book:

- [1] Ghosh MN. Fundamentals of Experimental Pharmacology, 2nd ed. Calcutta Scientific Book Agency, 1984:154.

Proofs will be sent to the corresponding author. These should be returned as quickly as possible.

The facts and view in the article will be of the authors and they will be totally responsible for authenticity, validity and originality etc. the authors should give an undertaking while submitting the paper that the manuscripts submitted to journal have not been published and have not been simultaneously submitted or published elsewhere and manuscripts are their original work.

www.jpc.stfindia.com
www.stfindia.com

Science – Tech Foundation

Journal of Pharmacy and Chemistry

(An International Research Journal of Pharmaceutical and Chemical Sciences)
(Indexing in CAS)

Plot No. 22, Vidyut Nagar, Anantapur – 515 001(A.P), INDIA

MEMBERSHIP FORM

Dear Editor,

I/We wish to be Annual Member / Life Member of Journal of Pharmacy and Chemistry (An International Research Journal of Pharmaceutical and Chemical Sciences) and agree to abide by your rules and regulations

1. Name in full: _____ Male ☐ Female ☐
(In block letters)
2. Nationality: _____ 3. Date of birth: _____
3. Corresponding Address: _____

5. Institutional / Business Address: _____
6. Phone : (O): _____ (R): _____ E-mail : _____
7. Academic Qualifications : _____
8. Profession and Experience : _____
9. Present Position / Post : _____
10. Pharmaceutical / Chemical interest: _____

Membership Fees	Life	Annual
Individual	Rs. 8000/- US \$ 800	Rs. 2000/- US \$ 150
Institutional	Rs. 20,000/- US \$ 2000	Rs. 2500/- US \$ 200

Rs. / \$ _____ remitted by Bank / Cash

DD No. _____ Date _____ Banker's Name _____

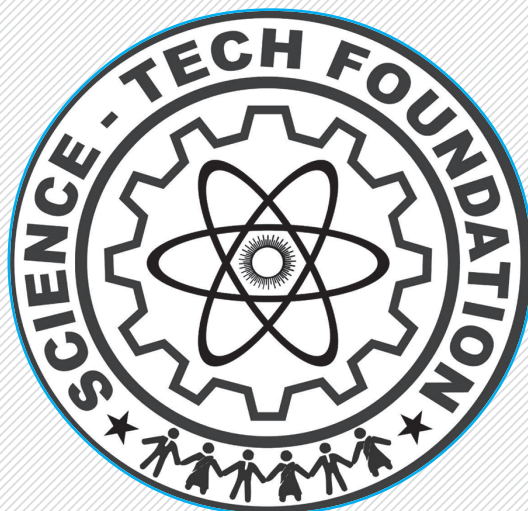
DD's are drawn in favour of **Science-Tech Foundation**, Payable at **Anantapur**.

Place: _____

Date: _____

(Signature of the applicant)

Note: (i) All authors should be member of this Journal, (ii) Saperate Photostat copy may be filled and send.



www.stfindia.com

Publications
JOURNAL OF PHARMACY AND CHEMISTRY
RESEARCH JOURNAL OF ENGINEERING AND TECHNOLOGY

Awards
FOR BEST B.Tech, B.Pharm., M.Tech., and M.Pharm. PROJECTS.

Best Teacher Award
FOR PROFESSIONAL TEACHERS

Scholarships
FOR POOR, BRIGHT AND TALENTED STUDENTS

Fellowships
FOR BRIGHT, POOR SCHOLARS OF ALL DISCIPLINES

Science-Tech Talent Test
FOR ALL STUDENTS

e-Lessons
FOR B.Tech. and B.Pharm. STUDENTS



Flat #105, First Floor, Block No: 1, Radiant Jasmine Gardens, Shivana Halli,
Jakkur Road, Yela Hanka, **BANGALORE** - 560064.

Flat # 401, Silver Springs, Street No.1, Czech Colony,
Sanath Nagar, **HYDERABAD** - 500018. A.P.



**2nd INTERNATIONAL CONFERENCE
ON
EMERGING TRENDS IN CHEMICAL AND PHARMACEUTICAL SCIENCES
On 15th - 17th October 2014**

REGISTRATION FORM

Title of the paper : _____

Name: _____

Designation: _____

Organization or Institution: _____

Department: _____

Address: _____

Phone: _____, Fax: _____,

E-Mail: _____

PLEASE TICK BELOW

I am likely to attend the International Conference : Yes [], No []

I intended to submit the paper : Yes [], No []

I would like to participate in exhibition : Yes [], No []

Abstract Enclosed : Yes [], No []

Accommodation needed : Yes [], No []

Registration fee enclosed : Yes [], No []

DETAILS OF REGISTRATION FEE

D.D. No _____ for Rs _____ dated _____ drawn in favour of "The
Science-Tech Foundation, payable at Hyderabad.

For online payment

Science Tech Foundation

A/c No. 50100031812242

HDFC Bank, RTGS/ NEFT IFSC: HDFC0002398 | SWIFT CODE : HDFCINBB

Note : Payment proof copy must be sent along with registration form.